Nitrobenzene Isomers

Miroslav Polášek and František Tureček*

Department of Chemistry, Bagley Hall, Box 351700, University of Washington, Seattle, Washington 98195-1700

Pascal Gerbaux† and Robert Flammang

Department of Chemistry, University of Mons-Hainaut, Mons, Belgium

Received: September 23, 2000; In Final Form: December 4, 2000

Several isomers of nitrobenzene (**1**) and nitrobenzene cation-radical (**1**$^{+\bullet}$) were identified as stable structures and their gas-phase chemistry was investigated by the methods of tandem mass spectrometry and combined ab initio and density functional theory calculations. The relative energies of $[C_6,H_5,N,O_2]$ neutral molecules followed the order *o*-nitrosophenol (**5**, most stable) < *p*-nitrosophenol (**7**) < *o*-benzoquinonenitrone (**10**) < *p*-benzoquinoneoxime (**19**) < *o*-benzoquinoneoxime (**11**) < *m*-nitrosophenol (**6**) < nitrobenzene (**1**) < phenyl nitrite (**8**) < benzo[*d*]-1,3-dioxa-2-azolidine (**13**) ≪ triplet didehydrocyclohexa-2,4-dien-1-yliden-1-nitronic acids, *para* ($^3A''$) **4**) ≈ *meta* ($^3A''$) anti-**3**) < *ortho* ($^3A''$) syn-**2**) < singlet didehydrocyclohexa-2,4-dien-1-yliden-1-nitronic acids, *meta* (^1A) syn-**3**) < *ortho* (^1A) syn-**2**) < *para* (^1A) **4**) (least stable). Molecules **1**, **5**, **7**, and **8**, were generated in the gas phase by femtosecond collisional electron transfer and their dissociations were investigated by neutralization-reionization mass spectrometry. The relative energies of $[C_6,H_5,N,O_2]^{+\bullet}$ cation radicals followed the order **7**$^{+\bullet}$(most stable) < **5**$^{+\bullet}$ < **6**$^{+\bullet}$ < anti-**11**$^{+\bullet}$ < **8**$^{+\bullet}$ < **10**$^{+\bullet}$ < **13**$^{+\bullet}$ < benzo-[*d*]-1,2-dioxa-3-azolidine (**12**$^{+\bullet}$) < **1**$^{+\bullet}$ < **4**$^{+\bullet}$ < syn-**3**$^{+\bullet}$ < syn-**2**$^{+\bullet}$ (least stable).

Introduction

Nitrobenzene (**1**) has been known since Mitscherlich's synthesis in 1834[1] and represents one of the classical compounds in organic chemistry that has been produced on an industrial scale since 1847.[2] Besides being an important solvent[3] and reagent,[4] **1** is an endothermic compound of a positive enthalpy of formation, $\Delta H°_{f,298} = 68.5$ kJ mol^{-1},[5] that has been used as a model compound in studies of reactions of energetic materials.[6] Photodissociation of nitrobenzene has been studied in detail[7] and phenyl nitrite has been suggested as an intermediate for photoinduced loss of NO.[8] However, with the exception of *p*-nitrosophenol, no stable aromatic isomers of neutral nitrobenzene are known.

We have observed recently[9] that the phenyl nitronic radical, a hydrogen atom adduct to the nitro group in **1**, underwent elimination of ring hydrogen atoms upon collisional excitation and ionization, indicating the possible formation of isomers **2**$^{+\bullet}$−**4**$^{+\bullet}$ of the nitrobenzene cation radical (Scheme 1). Ylid-ion isomers of several heterocyclic molecules have been prepared previously in the gas phase and found to be stable in the isolated state.[10] However, while the gas-phase chemistry of nitrobenzene cation-radicals has been studied extensively in the past,[11] no isomers have been positively identified and characterized.

The objective of this work was to generate ionic and neutral nitrobenzene isomers of the $[C_6,H_5,N,O_2]$ formula using the methods of gas-phase ion chemistry and study their structure, energetics, and reactivity by tandem mass spectrometry and high-level ab initio calculations. The gas-phase cation-radicals were used as precursors of transient molecules. The conversion

SCHEME 1

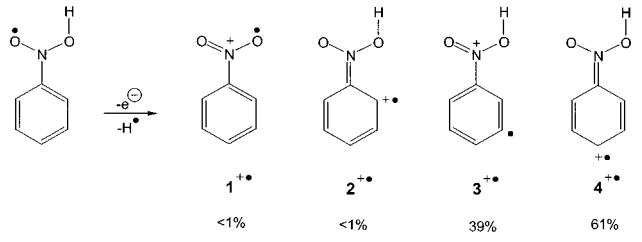

was achieved by collisional electron transfer from a thermal molecular electron donor to a cation-radical that has been accelerated to >110 000 m s^{-1} velocity resulting in a $<9 \times 10^{-15}$ s time for the collision event. Since this time is shorter than the vibrational periods of most molecular vibrations, the structure and geometry of the precursor ion is preserved in the nascent molecule.

The transient molecules are ionized after a few microseconds and analyzed by mass spectrometry. This neutralization−reionization mass spectrometric (NRMS)[12] method has been used to generate a wide variety of transient and highly reactive neutral species as reviewed.[13] Collisional activation of transient molecules (NCR)[14] was used to induce and probe their unimolecular dissociations. We also show by ab initio calculations that the thermochemistry of $[C_6,H_5,N,O_2]$ cation-radicals and molecules **1**-**19** spans a wide range of relative energies within which **1** and **1**$^{+\bullet}$ belong to the less stable species.

Experimental Part

Methods. Measurements of neutralization−reionization mass spectra were performed on the University of Washington tandem quadrupole acceleration−deceleration mass spectrometer (UW)

* Corresponding author. Tel: (206) 685-2041. Fax: (206) 685-3478. E-mail: turecek@chem.washington.edu.
† Chargé de Recherches du FNRS.

10.1021/jp003454r CCC: $20.00
Published on Web 01/18/2001

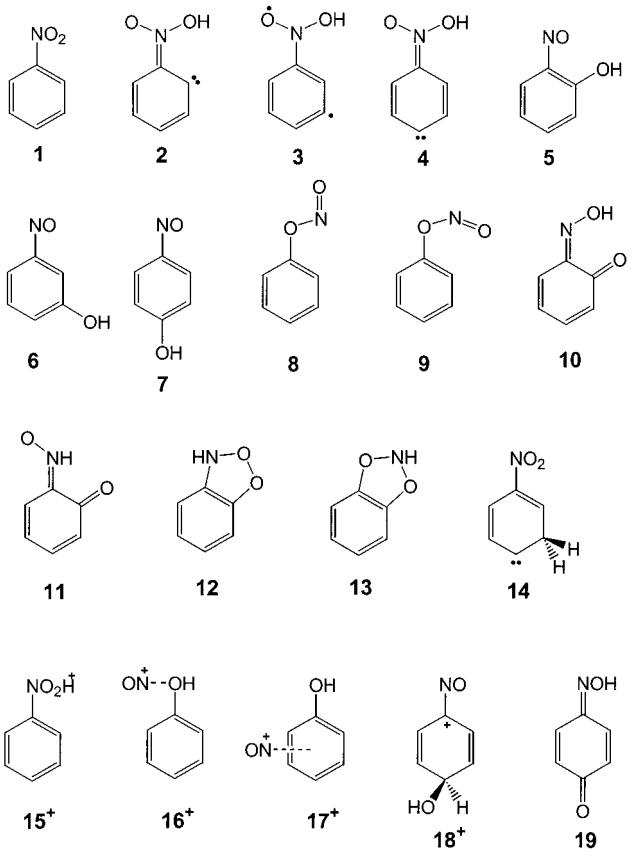

described previously[15] and on the University of Mons (UM) six-sector tandem mass spectrometer.[16]

In the UW measurements, collisionally activated dissociation (CAD) spectra were obtained on a JEOL HX-110 double focusing mass spectrometer of forward (electrostatic sector E precedes magnet B) geometry at 10 keV kinetic energy. Air was used as a collision gas that was admitted to the first field-free region at pressures to achieve 70 and 50% precursor ion beam transmittance. Dissociation products were monitored by linked scans in which B and E were scanned simultaneously while maintaining a constant B/E ratio. The mass resolution was >500 in these linked scans. Accurate mass measurements were also made on the JEOL HX-110 instrument at a resolving power $M/\Delta M > 10\,000$ (10% valley definition). Neutralization−reionization mass spectra were obtained on a tandem quadrupole acceleration−deceleration mass spectrometer that was described previously.[15] Cation-radicals were produced by electron ionization at 70 eV and 220−250 °C. Samples were introduced directly into the ion source from a glass probe to achieve pressures in the range of $(2-3) \times 10^{-6}$ Torr. Charge exchange ionization and ion−molecule reactions were performed in a tight ion source of our design. The pressure of the reagent gas was $(1-2) \times 10^{-4}$ Torr as read on the source diffusion pump intake. The ion source temperature was typically 280−320 °C. The ions were extracted from the ion source, passed through a quadrupole mass filter and accelerated to 8200 eV kinetic energy. Fast ions were allowed to collide with dimethyl disulfide that was admitted to the collision cell at pressures to achieve 70% transmission of the ion beam. Collisional activation of transient neutrals was performed in a 60-cm long drift region (conduit) to which helium was admitted at pressures allowing 70 or 50% ion beam transmittance. The conduit was floated at +250 V to reject any ions formed there. The flight time for the neutral intermediates was 5.3 μs on the UW instrument.. The neutral intermediates were reionized in a third collision cell to which O_2 was admitted at pressures to achieve 70% transmittance of the ion beam. The ions were decelerated to 75−80 eV, passed through an energy filter, and separated by a quadrupole mass analyzer that was operated at unit mass resolution. Spectra were accumulated over 30−50 consecutive scans.

The UM measurements were performed on a large-scale tandem mass spectrometer (Micromass AutoSpec 6F, Manchester) combining six sectors of $E_1c_1B_1c_2E_2c_3c_4E_3B_2c_5E_4$ geometry (E_i stands for electric sector, B_i for magnetic sector and c_i for collision cell).[16a] Typical conditions were 8 kV accelerating voltage, 200 μA trap current (in the electron ionization mode, EI), 1 mA (in the chemical ionization mode, methane CI), 70 eV ionizing electron energy, and 200 °C ion source temperature. Solid samples were introduced with a direct insertion probe; nitrobenzene was injected into the ion source via a heated (180 °C) septum inlet.

Collisionally activated dissociation (CAD) spectra of mass-selected ions of 8 keV kinetic energy were obtained with O_2 as collision gas in c_4. The CAD spectra were recorded by linked scanning of the fields of the three last sectors ($E_3B_2E_4$). The NR (Xe/O_2) unit is situated in the fourth field-free region, c_3 and c_4 being the neutralization and the reionization cells, respectively. The flight time for neutral intermediates was 0.7 μs on the UM instrument. The NR spectra were recorded by scanning the field of E_3.

The radio frequency-only quadrupole collision cell (Q_{coll}) between E_2 and E_3 has been reported previously.[16b] This modification allows one to study associative ion−molecule reactions and collisional activation of decelerated ions (ca. 20−30 eV kinetic energy). Briefly, a beam of fast ions (8 keV) is selected with the three first sectors ($E_1B_1E_2$) and decelerated to approximately 5 eV (to maximize ion−molecule reactions) or 20−30 eV (to maximize collision-induced dissociations). Reactions between the ions and the reagent gas (the pressure of the gas is estimated to be about 10^{-3} Torr) are conducted in Q_{coll} and, after acceleration to 8 keV, the ions generated in the quadrupole are separated by scanning the field of the second magnet. The high-energy CAD spectra of mass-selected ions generated in the Q_{coll} can be recorded by a linked scan of the fields of the last three sectors.

In the MS/MS/MS experiments, fast (8 keV) mass-selected ions are decelerated to 20−30 eV and fragmented by collision with argon in the Q_{coll}. After acceleration to 8 keV, fragment ions of interest are selected by E_3B_2, submitted to collision with nitrogen in the last cell (c_5), and the CAD spectrum is then recorded in the usual way (E scan).

Materials. Nitrobenzene, *o*-dinitrobenzene, *m*-dinitrobenzene, *p*-dinitrobenzene, phenol, *o*-nitrobenzoic acid, *o*-nitroacetophenone, and *p*-nitrosophenol (all Aldrich) were used as received. Methyl nitrite and methyl-d_3 nitrite were prepared from methanol and CD_3OD, respectively, according to the literature procedure.[17] Attempted syntheses of *o*-nitrosophenol (**5**) by copper acetate catalyzed oxidation of benzene or phenol according to the published procedures[18] were unsuccessful in our hands and did not result in a well-defined product. An attempted synthesis of phenyl nitrite (**8**) by esterification of phenol with neat *n*-propyl nitrite under catalysis of 5% mol *p*-toluenesulfonic acid at 0 °C yielded only tars and traces of *o*-nitrophenol.

Calculations. Standard ab initio calculations were performed using the Gaussian 98 suite of programs.[19] Geometries were optimized with density functional calculations[20] that employed Becke's hybrid functional (B3LYP)[21] and the 6-31+G(d,p) basis set. Stationary points were characterized by harmonic frequency analysis as local minima (all frequencies real) or first-order

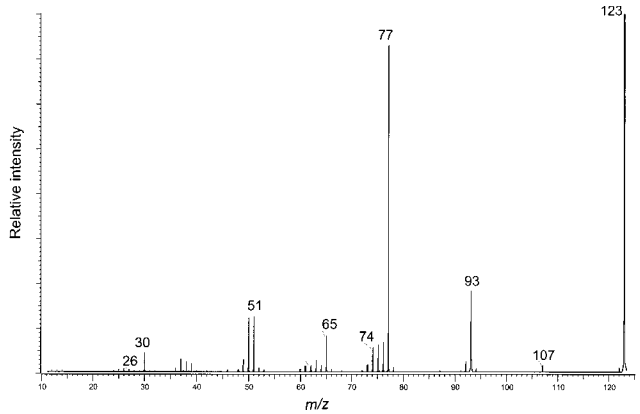

Figure 1. Collisionally activated dissociation (10 keV, air, 70% transmittance) spectrum of nitrobenzene cation-radical $\mathbf{1}^{+\bullet}$.

saddle points (one imaginary frequency). The B3LYP frequencies were scaled by 0.963[22] (for other scaling factors see refs 23−25). Single-point energies were obtained with B3LYP and Møller−Plesset perturbational calculations with valence electron-only excitations that were truncated at second order (MP2, frozen core), using the larger 6-311+G(2df,p) and 6-311+G-(3df,2p) basis sets. Spin unrestricted UB3LYP and UMP2 calculations were used for open-shell species. The UMP2 calculations showed substantial spin contamination as judged from the $\langle S^2 \rangle$ expectation values that were 0.77−1.79. These were partially corrected by Schlegel's spin annihilation procedure[26] that lowered the total energies by 2−69 millihartree and resulted in $\langle S^2 \rangle$ values of 1.15−0.75. To further deal with the spin contamination problem we used restricted open-shell Møller−Plesset calculations[27] (ROMP2) that were recently suggested for ill-behaving radical systems.[28] The projected (PMP2) and ROMP2 energies were averaged with the B3LYP energies in an empirical correction procedure denoted as B3-PMP2 and B3-ROMP2, respectively. We have shown previously that averaging the B3LYP and MP2 relative energies resulted in efficient cancellation of small errors pertinent to these formalisms and provided excellent relative energies, proton affinities, acidities, ionization energies, and electron affinities for a number of systems.[29−31]

Results and Discussion

Preparation of $[C_6,H_5,N,O_2]^{+\bullet}$ Cation Radicals. The cation radical $\mathbf{1}^{+\bullet}$ was generated by electron and charge-exchange ionization of nitrobenzene. The ion has been studied in detail previously and its metastable-ion[11b,11k] and high-energy CAD mass spectra[9a] were reported. A reference CAD spectrum is shown in Figure 1. Other ion isomers with the $[C_6,H_5,N,O_2]$ composition were generated as follows.

Ylid Ions $\mathbf{2}^{+\bullet}$−$\mathbf{4}^{+\bullet}$. *ortho*-, *meta*-, and *para*-Dinitrobenzenes were protonated selectively in one of the nitro groups that represent the most basic centers in the corresponding molecules (Scheme 2). The protonated dinitrobenzenes showed distinct CAD spectra (Figures 2a−4a) that proved that the isomeric structures were preserved upon protonation. Collisional activation of nitroaromate cations often results in loss of NO_2;[32] CAD of protonated dinitrobenzenes was therefore expected to yield ions $\mathbf{2}^{+\bullet}$−$\mathbf{4}^{+\bullet}$. For $\mathbf{2}^{+\bullet}$ and $\mathbf{3}^{+\bullet}$ both syn- and *anti*-conformers can be produced (Scheme 2) that were unresolved by experiment but were characterized by theory (vide infra). The corresponding protonated dinitrobenzene cations of *m*/*z* 169 were selected by mass and subjected to collision activation with Ar at low (30 eV) kinetic energies (Figures 2a−4a). For all three isomers, loss

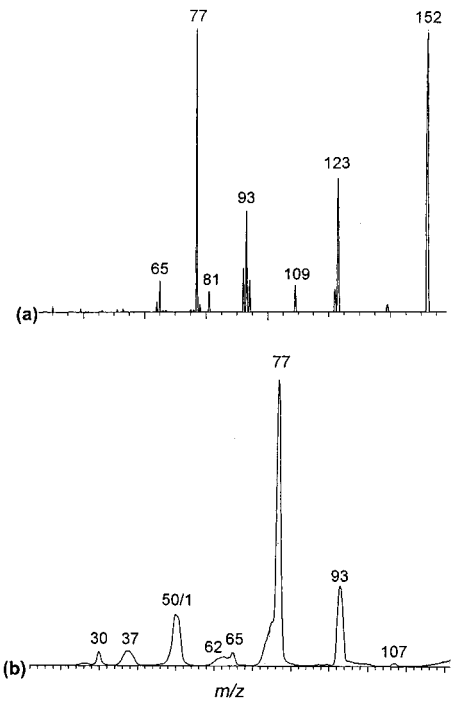

Figure 2. (a) Low energy (Ar, 30 eV) CAD spectrum of protonated *o*-dinitrobenzene. (b) High-energy (O_2, 8 keV) CAD spectrum of mass-selected *m*/*z* 123 ion from Figure 2a.

SCHEME 2

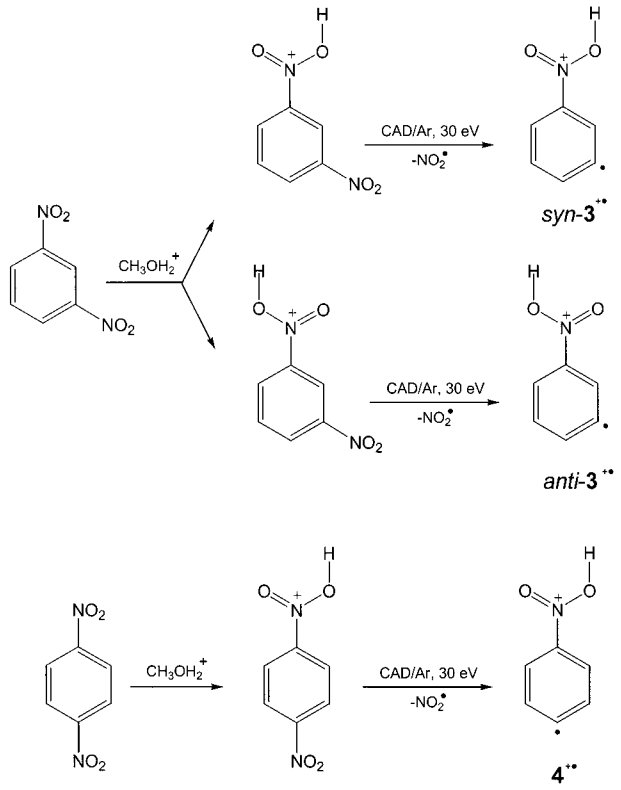

of NO_2 produced fragment ions at *m*/*z* 123 which were most abundant when formed from the *ortho*-isomer. The dissociation products were mass separated to select the *m*/*z* 123 ions that were accelerated to 8 keV and further probed by CAD. These CI-CAD-low-eV/CAD-keV spectra are shown in Figures 2b−4b. The CI-CAD/CAD spectrum of $\mathbf{2}^{+\bullet}$ (Figure 2b) was very similar to that of $\mathbf{1}^{+\bullet}$ (Figure 1) and showed fragments formed by loss of O (*m*/*z* 107), NO (*m*/*z* 93), NO_2 (*m*/*z* 77), and ions of

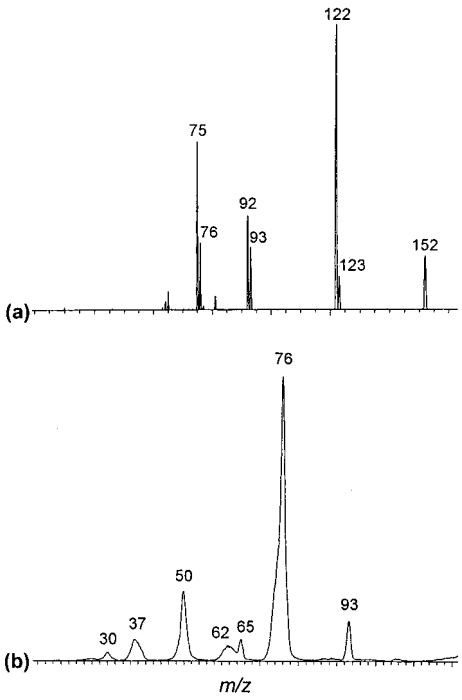

Figure 3. (a) Low energy (Ar, 30 eV) CAD spectrum of protonated *m*-dinitrobenzene. (b) High-energy (O_2, 8 keV) CAD spectrum of mass-selected *m*/*z* 123 ion $\mathbf{3}^{+\bullet}$ from Figure 3a.

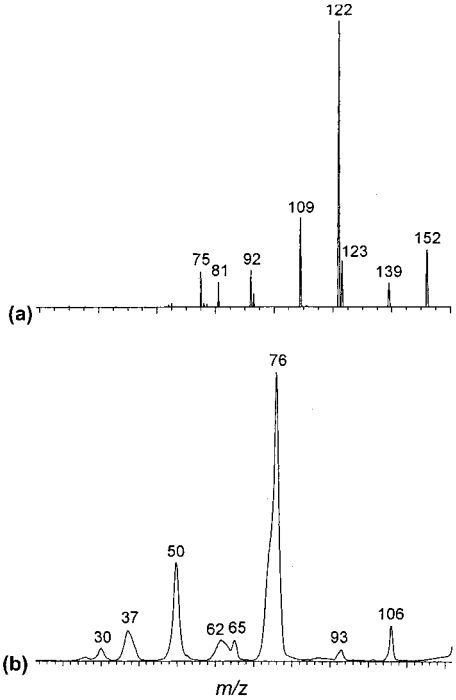

Figure 4. (a) Low energy (Ar, 30 eV) CAD spectrum of protonated *p*-dinitrobenzene. (b) High-energy (O_2, 8 keV) CAD spectrum of mass-selected *m*/*z* 123 ion $\mathbf{4}^{+\bullet}$ from Figure 4a.

the aromatic series[33] at *m*/*z* 65, 50, and 37. By contrast, the CI-CAD/CAD spectra of $\mathbf{3}^{+\bullet}$ and $\mathbf{4}^{+\bullet}$ differed from that of $\mathbf{1}^{+\bullet}$ and from each other as well (Figure 3b, 4b). In particular, the spectrum of $\mathbf{3}^{+\bullet}$ showed a peak at *m*/*z* 76 that was formed by loss of HONO from the precursor ion. The spectrum of $\mathbf{4}^{+\bullet}$ showed an *m*/*z* 106 peak (loss of OH), and an *m*/*z* 76 peak by loss of HONO. These dissociations were compatible with the presence of an NO_2H group in $\mathbf{3}^{+\bullet}$ and $\mathbf{4}^{+\bullet}$ and pointed to ylid-ion structures, $C_6H_4-NO_2H^{+\bullet}$, for the ions. It may be noted that CAD of protonated chloro, bromo, and iodonitrobenzenes were also investigated but did not produce significant yields of *m*/*z* 123 ions corresponding to $\mathbf{2}^{+\bullet}-\mathbf{4}^{+\bullet}$.

Phenyl Nitrite Ions $\mathbf{8}^{+\bullet}/\mathbf{9}^{+\bullet}$. A yet different $[C_6,H_5,N,O_2]^{+\bullet}$ ion was generated by ion−molecule reactions in a gaseous phenol−methyl nitrite−methanol mixture under conditions of chemical ionization (CI).[34] CI with methyl nitrite−methanol generates the $CH_3O(H)NO^+$ [35] and $CH_3O(NO)_2^+$ ions[36] that can be used for gas-phase nitrosation.[9a] However, the CI spectrum of phenol showed the presence of $C_6H_5OH^{+\bullet}$ (*m*/*z* 94), $CH_3O(NO)_2^+$ (*m*/*z* 91) that was shifted to *m*/*z* 94 when CD_3-ONO was used, $[C_6,H_5,N,O_2]^{+\bullet}$ (*m*/*z* 123), NO^+ (*m*/*z* 30), and $CH_3O(H)NO^+$ (*m*/*z* 62) ions, whereas the expected product of NO^+ addition to phenol (*m*/*z* 124) was a minor component (Figure 5a). The energetics of this unusual phenol nitrosation in the gas phase is discussed later in the paper. The elemental composition and homogeneity of the *m*/*z* 123 peak was confirmed by a high-resolution CI mass spectrum. The CAD spectrum of the *m*/*z* 123 ion (Figure 5b) was distinctly different from those of the other isomers $\mathbf{1}^{+\bullet}-\mathbf{4}^{+\bullet}$. In particular, the CAD spectrum showed a dominant peak due to loss of NO (*m*/*z* 93), whereas the *m*/*z* 107, 106, 95, 77, and 76 peaks were negligible. We assign this ion the structure of phenyl nitrite ($\mathbf{8}^{+\bullet}$ or $\mathbf{9}^{+\bullet}$).

Ion−molecule reactions were also conducted with mass-selected $C_6H_5OH^{+\bullet}$ ions that were allowed to react with gaseous *tert*-butyl nitrite in the quadrupole collision cell at 3−5 eV laboratory kinetic energy. The reaction produced an ion at *m*/*z* 123 (Figure 6a) that was mass-selected, accelerated to 8 keV, and

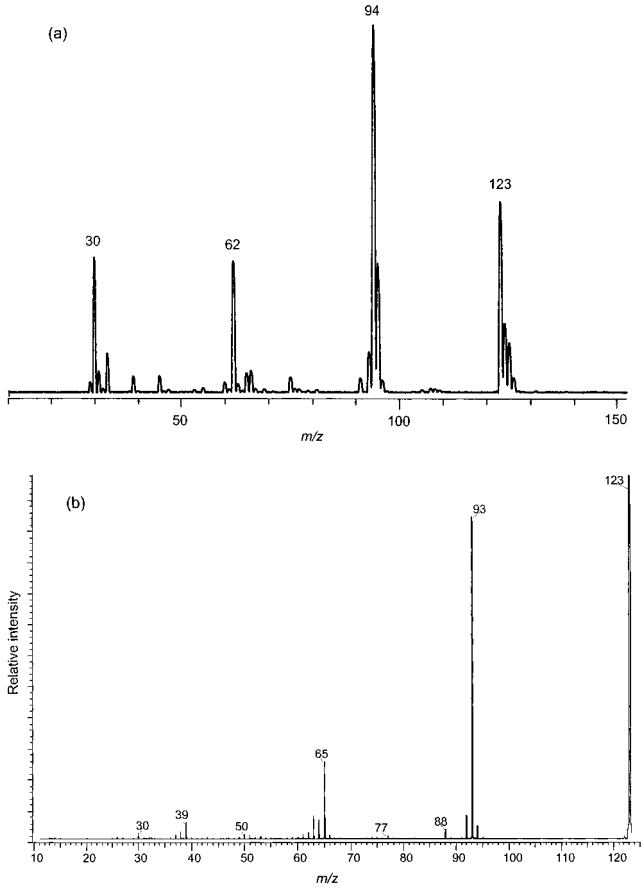

Figure 5. (a) Chemical ionization mass spectrum of mixture of methyl nitrite, methanol, and phenol. (b) CAD (10 keV, air, 70% transmittance) of the *m*/*z* 123 ion ($\mathbf{8}^{+\bullet}/\mathbf{9}^{+\bullet}$).

probed by CAD. The CAD spectrum showed dissociations that were characteristic of ions $\mathbf{8}^{+\bullet}$ or $\mathbf{9}^{+\bullet}$, e.g., the dominant loss of NO (*m*/*z* 93) and negligible *m*/*z* 106 and 77 peaks (Figure 6b).

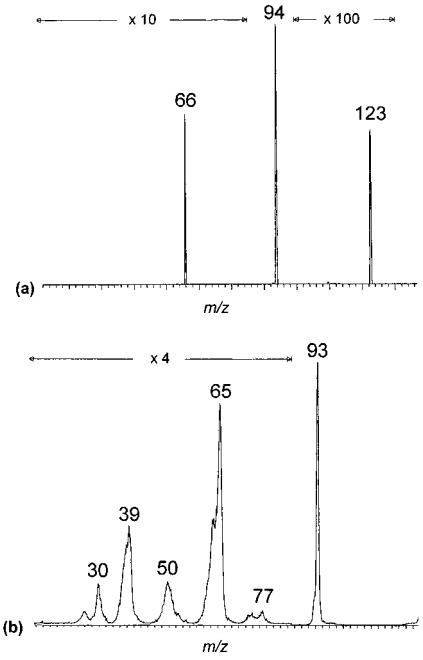

Figure 6. (a) Mass spectrum of the products of the ion−molecule reaction of mass-selected $C_6H_5OH^{+\bullet}$ with *tert*-butyl nitrite at 3−5 eV laboratory kinetic energy. (b) CAD (8 keV, O_2, 70% transmittance) of *m*/*z* 123 ion from the above ion−molecule reaction.

$[C_6,H_5,N,O_2]^{+\bullet}$ Ions by Dissociative Ionization. A third mode of synthesizing $[C_6,H_5,N,O_2]^{+\bullet}$ cation-radicals was by dissociative ionization of *o*-nitrobenzoic acid[11f] and *o*-nitroacetophenone.[11g] The CAD spectra of these ions are shown in Figure 7. The *m*/*z* 123 ion from *o*-nitrobenzoic acid gave a CAD spectrum (Figure 7a) that was very similar to that of $\mathbf{1}^{+\bullet}$ regardless of whether the ion was generated in the ion source or by dissociations of metastable *o*-nitrobenzoic cation-radical. This finding contradicts an early report by Benoit and Holmes[11f] who assigned the *m*/*z* 123 ion from *o*-nitrobenzoic acid the structure of phenyl nitrite ($\mathbf{8}^{+\bullet}$).

CAD of the *m*/*z* 123 ion from *o*-nitroacetophenone resulted in a dominant loss of OH (*m*/*z* 106) and less prominent losses of CO (*m*/*z* 95) and NO (*m*/*z* 93), whereas losses of NO_2 and HONO were negligible (Figure 7b). Loss of OH also dominated dissociations of metastable *m*/*z* 123 ions from *o*-nitroacetophenone. Finally, *m*/*z* 123 ions produced by dissociations of metastable *o*-nitroacetophenone cation-radical produced a CAD spectrum which was indistinguishable from that corresponding to ions formed by a more energetic dissociation in the ion source.

The mass-selected $[C_6,H_5,N,O_2]^{+\bullet}$ ions from nitrobenzene and *o*-nitroacetophenone were further investigated through ion−molecule reactions with NO and CH_3SSCH_3 at low collision energies in the collision quadrupole of the UM instrument.[16b] CH_3SSCH_3 is known to react with radical centers in distonic ions, and the reaction provides a useful probe of ion structures.[37] Ion $\mathbf{1}^{+\bullet}$ underwent exclusive charge exchange with NO and CH_3SSCH_3 in keeping with the corresponding ionization energies, IE(**1**) = 9.84 eV, IE(NO) = 9.25 eV, and IE(CH_3SSCH_3) = 8.1 eV[5] that made the electron-transfer exothermic for both reagent gases. In contrast, the $[C_6,H_5,N,O_2]^{+\bullet}$ ion from *o*-nitroacetophenone was unreactive to NO indicating that the corresponding $[C_6,H_5,N,O_2]$ neutral had IE < 9.25 eV. Reaction with CH_3SSCH_3 proceeded by electron transfer that indicated that the $[C_6,H_5,N,O_2]^{+\bullet}$ ion had a recombination energy close to 8.0 eV or contained a component of such a property.

Finally, a yet different ion $\mathbf{7}^{+\bullet}$ was prepared by electron ionization of stable *p*-nitrosophenol, and its CAD spectrum was

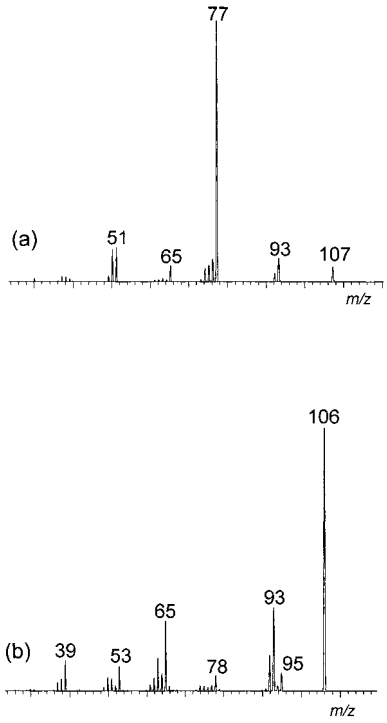

Figure 7. CAD (8 keV, O_2, 70% transmittance) of (a) *m*/*z* 123 ion from *o*-nitrobenzoic acid and (b) *m*/*z* 123 ion from *o*-nitroacetophenone.

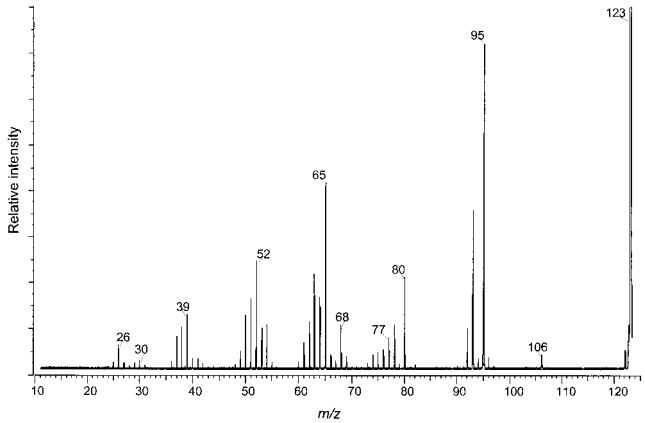

Figure 8. CAD (10 keV, air, 70% transmittance) of *p*-nitrosophenol ion $\mathbf{7}^{+\bullet}$.

recorded for reference. The CAD spectrum showed a weak losses of CO (*m*/*z* 95.0369, C_5H_5NO) and NO (*m*/*z* 93.0343, C_6H_5O), elimination of C_2H_3O (*m*/*z* 80.0141, C_4H_2NO), and fragments of the aromatic series (Figure 8). The CAD spectrum of $\mathbf{7}^{+\bullet}$ was distinctly different from those of the other ion isomers. In particular the presence of the *m*/*z* 80 peak was unique for ion $\mathbf{7}^{+\bullet}$ and its absence in the CAD spectra of the other ion isomers indicated that they did not isomerize to the very stable ion $\mathbf{7}^{+\bullet}$.

In summarizing the ion synthesis part, we proved through CAD spectra and ion−molecule reactions the existence of six distinct $[C_6,H_5,N,O_2]^{+\bullet}$ cation-radicals. The structures, relative energies, and dissociation energetics of the $[C_6,H_5,N,O_2]^{+\bullet}$ isomers were further investigated by ab initio and density functional calculations.

Ion Structures and Energies. Several $[C_6,H_5,N,O_2]^{+\bullet}$ cation-radicals were found by B3LYP/6-31+G(d,p) geometry optimizations to exist as equilibrium structures in local energy minima (Figure 9). The ion structures mostly showed unexceptional bond lengths and angles. The *syn*- and *anti*-rotamers of $\mathbf{2}^{+\bullet}$ and $\mathbf{3}^{+\bullet}$

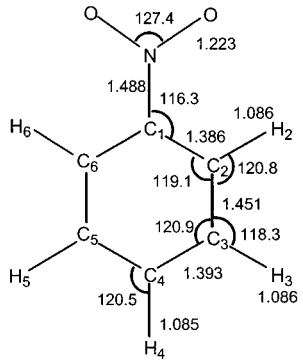

1$^{+\bullet}$ (C_{2v})

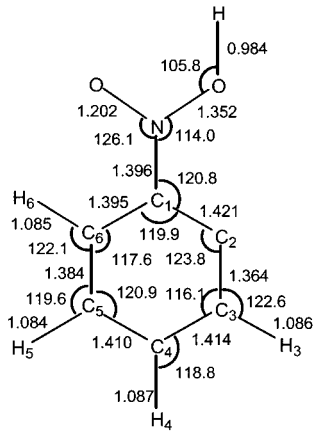

syn-**2**$^{+\bullet}$ (C_s)

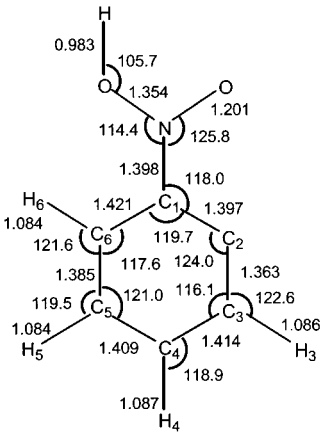

anti-**2**$^{+\bullet}$ (C_s)

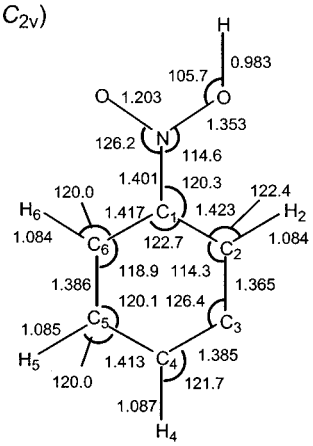

syn-**3**$^{+\bullet}$ (C_s)

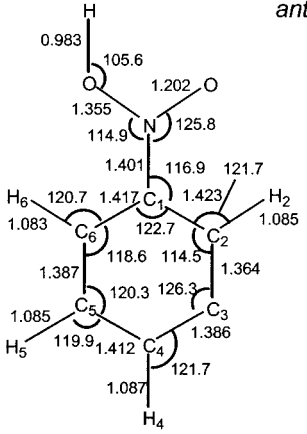

anti-**3**$^{+\bullet}$ (C_s)

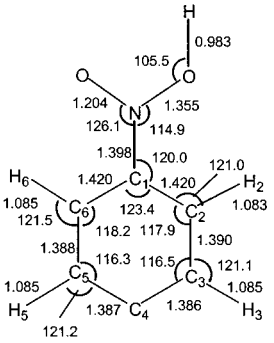

4$^{+\bullet}$ (C_s)

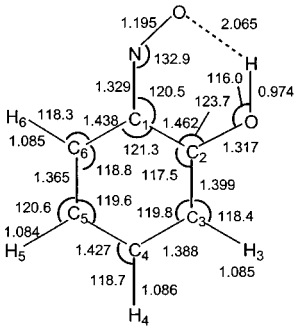

5$^{+\bullet}$ (C_s)

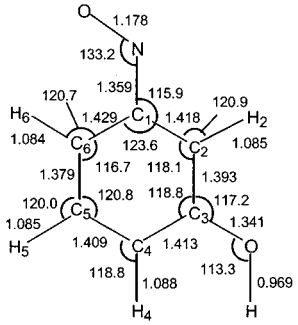

6$^{+\bullet}$ (C_s)

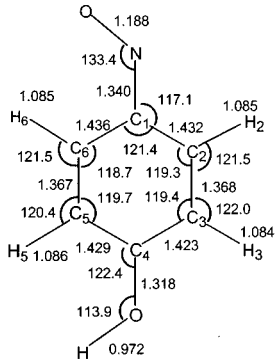

7$^{+\bullet}$ (C_s)

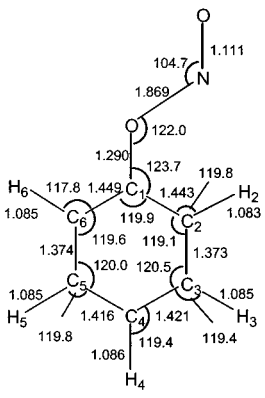

8$^{+\bullet}$ (C_s)

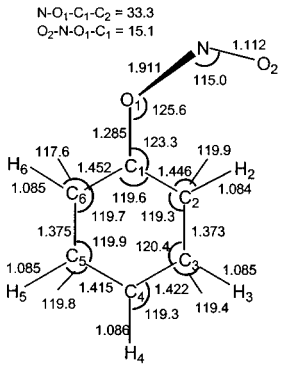

9$^{+\bullet}$

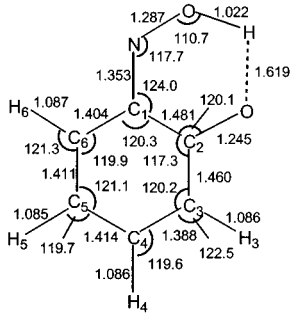

10$^{+\bullet}$ (C_s)

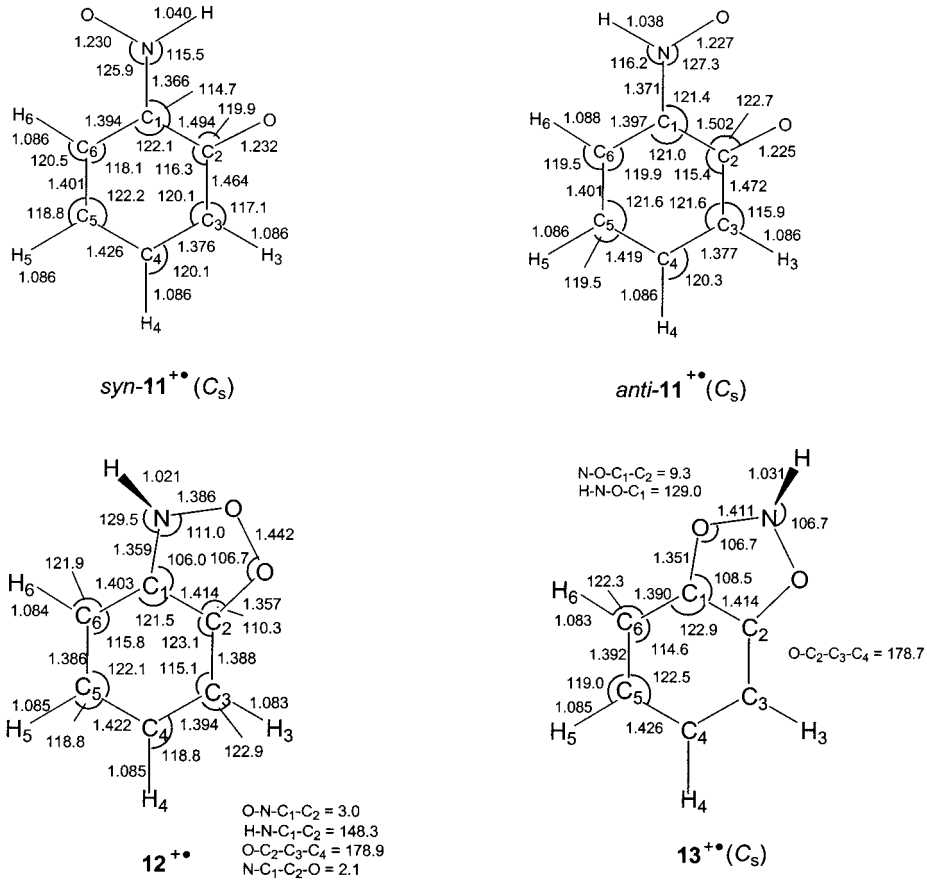

Figure 9. B3LYP/6-31+G(d,p) optimized structures of $[C_6,H_5,N,O_2]^{+\bullet}$ cation-radicals. Bond lengths in angstroms, bond and dihedral angles in degrees.

TABLE 1: Ion Energies

	relative energy[a]					
ion	B3LYP/ 6-31+G(d,p)	B3LYP/ 6-311+G(2df,p)	PMP2/ 6-311+G(2df,p)	ROMP2/ 6-311+G(2df,p)	B3-PMP2	B3-ROMP2
1$^{+\bullet}$	0	0	0	0	0	0
syn-**2**$^{+\bullet}$	43	40	48	49 (49)[b]	44	44
TS(**1**$^{+\bullet}$ → *syn*-**2**$^{+\bullet}$)	116	111	147	117 (120)[b]	129	114
anti-**2**$^{+\bullet}$	46	43	52		48	
syn-**3**$^{+\bullet}$	44	41	51	45	46	43
anti-**3**$^{+\bullet}$	44	41	51		46	
4$^{+\bullet}$	40	37	48	43	42	40
5$^{+\bullet}$	−204	−209	−172	−172	−191	−190
6$^{+\bullet}$	−189	−195	−165	−175	−180	−185
7$^{+\bullet}$	−233	−239	−204	−197	−221	−218
8$^{+\bullet}$	−142	−151	−151	−155 (−153)[b]	−151	−153
9$^{+\bullet}$	−122	−130	−128	−134	−129	−132
TS(**1**$^{+\bullet}$ → **9**$^{+\bullet}$)	112	109	110	114 (115)[b]	110	111
10$^{+\bullet}$	−142	−138	−103	−107	−121	−123
anti-**11**$^{+\bullet}$	−160	−158	−132	−153	−145	−156
syn-**11**$^{+\bullet}$	−131	−131	−100	−124	−115	−127
12$^{+\bullet}$	−20	−22	15	−4	−4	−13
13$^{+\bullet}$	−98	−100	−69	−75	−84	−88
14$^{+\bullet}$	162	160	174	174	167	167

[a] In units of kJ mol^{-1} at 0 K. [b] From single point-calculations with the 6-311+G(3df,2p) basis set.

had very similar structures (Figure 9) and energies (Table 1). The O−N bonds in phenyl nitrite ions **8**$^{+\bullet}$ and **9**$^{+\bullet}$ were conspicuously long and indicated facile dissociation (vide infra). According to the calculated relative stabilities, the ion isomers can be divided into three groups. The nitrobenzene cation radical **1**$^{+\bullet}$, ylid-ion isomers **2**$^{+\bullet}$−**4**$^{+\bullet}$ and **14**$^{+\bullet}$, and the benzo[*d*]-1,2-dioxa-3-azolidine ion **12**$^{+\bullet}$ represented the least stable group of ions. Interestingly, the nonclassical ylid-ions **2**$^{+\bullet}$−**4**$^{+\bullet}$ were only slightly destabilized with respect to **1**$^{+\bullet}$ (Table 1). Ylid-ions formed by 1,2-hydrogen migrations within the benzene ring were also addressed by calculations but were found to be very high energy structures, e.g., ion **14**$^{+\bullet}$ (Table 1). The phenyl nitrite rotamers **8**$^{+\bullet}$ and **9**$^{+\bullet}$, *o*-benzoquinone oxime (**10**$^{+\bullet}$) and nitrone (*syn*-**11**$^{+\bullet}$ and *anti*-**11**$^{+\bullet}$) ions, and the benzo[*d*]-1,3-dioxa-2-azolidine ion **13**$^{+\bullet}$ represented a second group of stable ion isomers. The most stable ion isomers consisted of nitrosophenol ions **5**$^{+\bullet}$− **7**$^{+\bullet}$ that were 180−220 kJ mol^{-1} more stable than **1**$^{+\bullet}$, with **7**$^{+\bullet}$ being the global energy minimum.

TABLE 2: Ion Dissociation Energies

reaction	dissociation energy[a] B3LYP/ 6-31+G(d,p)	B3LYP/ 6-311+G(2df,p)	PMP2/ 6-311+G(2df,p)	ROMP2/ 6-311+G(2df,p)	B3−PMP2	B3−ROMP2
$\mathbf{1}^{+\bullet} \rightarrow C_6H_5^+ + NO_2^\bullet$	138	128	137	137 (140)[b]	133	133 (135)[c]
$\mathbf{1}^{+\bullet} \rightarrow C_6H_5O^+ + NO^\bullet$	−40	−41	−20	−20	−31	−31 (−28)[c]
$\mathbf{1}^{+\bullet} \rightarrow C_6H_5O^\bullet + NO^+$	84	66	16	5	41	35
$\mathbf{8}^{+\bullet} \rightarrow C_6H_5O^+ + NO^\bullet$	102	109	131	135	120	122 (124)[c]
syn-$\mathbf{2}^{+\bullet} \rightarrow$ *o*-$C_6H_4^{+\bullet}$ + *anti*-HONO	247	245	275	262	260	253
syn-$\mathbf{2}^{+\bullet} \rightarrow$ (^3A) *o*-$C_6H_4NO^+ + OH^\bullet$	227	229	305		267	
syn-$\mathbf{2}^{+\bullet} \rightarrow$ (^1A) *o*-$C_6H_4NO^+ + OH^\bullet$	270	268	312	323	290	295
TS(*syn*-$\mathbf{2}^{+\bullet} \rightarrow \mathbf{1}^{+\bullet}$)	73	71	99	68 (71)[b]	85	70
$\mathbf{4}^{+\bullet} \rightarrow$ *p*-$C_6H_4^{+\bullet}$ + *anti*-HONO	261	258	317	315	288	286
$\mathbf{4}^{+\bullet} \rightarrow$ (^3A) *p*-$C_6H_4NO^+ + OH^\bullet$	222	223	285	292	254	258
$\mathbf{4}^{+\bullet} \rightarrow$ (^1A) *p*-$C_6H_4NO^+ + OH^\bullet$	275	276	295	310	285	293
$C_6H_5NO_2H^+ \rightarrow$ *syn*-$\mathbf{2}^{+\bullet} + H^\bullet$	474	469	479	468	474	468
$C_6H_5NO_2H^+ \rightarrow \mathbf{7}^{+\bullet} + H^\bullet$	201	193	228	229	211	211

[a] In units of kJ mol^{-1} at 0 K. [b] From ROMP2/6-311+G(3df,2p) single-point calculations. [c] 298 K values.

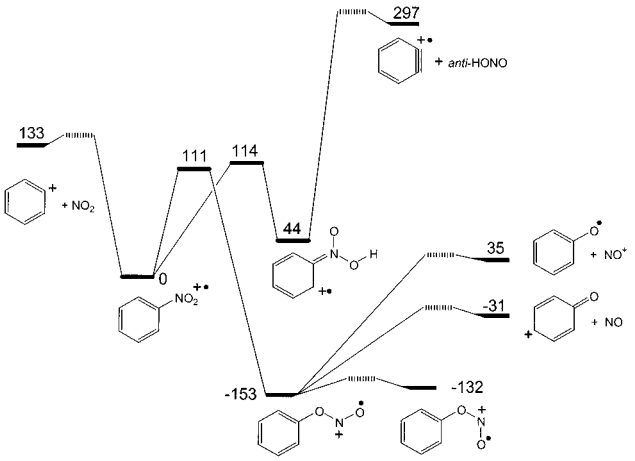

Figure 10. B3-ROMP3/6-311+G(2df,p) potential energy diagram for dissociations and isomerizations of ion $\mathbf{1}^{+\bullet}$.

Dissociations of Nitrobenzene Ion $\mathbf{1}^{+\bullet}$. An important feature of the chemistry of $\mathbf{1}^{+\bullet}$− $\mathbf{14}^{+\bullet}$is the energetics of ion isomerizations and dissociations (Table 2). Ion $\mathbf{1}^{+\bullet}$ was calculated to be metastable with respect to exothermic dissociation to $C_6H_5O^+$ + NO. Formation of the complementary pair of products, $C_6H_5O^\bullet + NO^+$, was calculated to be 35 kJ mol^{-1} endothermic and represented another low-energy dissociation of $\mathbf{1}^{+\bullet}$. Both dissociations proceed with isomerization to the more stable phenyl nitrite ions $\mathbf{8}^{+\bullet}$ or $\mathbf{9}^{+\bullet}$. This mechanism was established previously by Benoit and Holmes who used [1-^{13}C]-labeled nitrobenzene.[11g] The present calculations indicate that $\mathbf{8}^{+\bullet}$ is separated from $\mathbf{1}^{+\bullet}$ by a potential energy barrier of 111 kJ mol^{-1} (Table 2). Isomerization $\mathbf{1}^{+\bullet} \rightarrow \mathbf{8}^{+\bullet}$ thus represents a rate-determining step in the dissociation to $C_6H_5O^+$ + NO, because the intermediate ion $\mathbf{8}^{+\bullet}$ is formed with 264 kJ mol^{-1} internal energy (142 kJ mol^{-1} above the dissociation threshold) and is expected to dissociate rapidly. The B3-ROMP2 transition state and dissociation energies are visualized in a potential energy diagram (Figure 10).

Endothermic isomerization $\mathbf{1}^{+\bullet} \rightarrow \mathbf{2}^{+\bullet}$ also proceeded over a barrier (114 kJ mol^{-1}) that was comparable to that for isomerization to $\mathbf{8}^{+\bullet}$. However, further dissociations of $\mathbf{2}^{+\bullet}$ were all substantially endothermic, whereas the barrier for the reverse isomerization to $\mathbf{1}^{+\bullet}$ was low (Table 2). Therefore, ylid-ion $\mathbf{2}^{+\bullet}$ represents a kinetic cul-de-sac and should not participate as an intermediate in dissociations of $\mathbf{1}^{+\bullet}$ (Figure 10).

Dissociation of $\mathbf{1}^{+\bullet}$ to $C_6H_5^+ + NO_2$ required a threshold energy that was somewhat higher than the barrier for isomerization to $\mathbf{8}^{+\bullet}$ (Figure 10). Because of the nature of these competing reactions (direct bond cleavage versus rearrangement), the dissociation kinetics of $\mathbf{1}^{+\bullet}$ was expected to show a crossover of $k(E)$ curves for the isomerization and direct bond cleavage at an energy above the 133 kJ mol^{-1} threshold for the latter dissociation. Dissociations of $\mathbf{1}^{+\bullet}$ having internal energies between 114 kJ mol^{-1} and that for the crossover point will be dominated by the formation of $C_6H_5O^+ + NO$, while the formation of $C_6H_5^+ + NO_2$ will take over at higher internal energies. It is interesting to note that both the electron-induced dissociations and CAD of $\mathbf{1}^{+\bullet}$ showed that the formation of $C_6H_5^+ + NO_2$ was favored by a 4:1 ratio, whereas metastable $\mathbf{1}^{+\bullet}$ dissociated to $C_6H_5O^+ + NO$.[11b,l] This can be explained taking into account the internal energy distribution in $\mathbf{1}^{+\bullet}$, as estimated from the available electronic states of the ion from the photoelectron spectrum (PES) of nitrobenzene.[38] The PES showed a band of the *X* state at 9.92 eV and the bands of the *A, B,* and C states at 11.03,11.22, and 12.74 eV, respectively. If populated by ionization or collisional activation, the *A* state provides 107 kJ mol^{-1} internal energy which is below the lowest dissociation threshold of $\mathbf{1}^{+\bullet}$, the *B* state (125 kJ mol^{-1}) is metastable with respect to isomerization to $\mathbf{8}^{+\bullet}$, but does not have enough energy for dissociation to $C_6H_5^+ + NO_2$, and the *C* state (272 kJ mol^{-1}) is dissociative. The calculated isomerization and dissociation energies thus explained very well the observed competition between the dissociation channels in metastable $\mathbf{1}^{+\bullet}$ and following collisional activation.[11b,h,l]

Formation and Dissociations of Phenyl Nitrite Ions $\mathbf{8}^{+\bullet}$ and $\mathbf{9}^{+\bullet}$. The calculated energies also indicated that loss of NO should be the kinetically preferred dissociation of the phenyl nitrite ions $\mathbf{8}^{+\bullet}$ and $\mathbf{9}^{+\bullet}$. This is best compatible with the metastable-ion and CAD spectra of the ion prepared by CH_3-ONO chemical ionization of phenol which is therefore assigned structure $\mathbf{8}^{+\bullet}$. The energetics of the ion−molecule reactions that gave rise to $\mathbf{8}^{+\bullet}$ and included the species present in the CI mixture are shown in eqs 1−3:

$$C_6H_5OH + CH_3O(NO)_2^+ \rightarrow \textit{anti}\text{-}C_6H_5ONO^{+\bullet} + CH_3O{-}NH{-}O^\bullet \qquad \Delta H_{rxn,298} = 154 \text{ kJ mol}^{-1} \quad (1)$$

$$C_6H_5OH + CH_3O(NO)_2^+ \rightarrow \textit{anti}\text{-}C_6H_5ONO^{+\bullet} + CH_3O{-}N{-}OH^{\bullet} \quad \Delta H_{rxn,298} = 153 \text{ kJ mol}^{-1} \quad (2)$$

$$C_6H_5OH^{+\bullet} + \textit{syn}\text{-}CH_3ONO \rightarrow \textit{anti}\text{-}C_6H_5ONO^{+\bullet} + CH_3OH \quad \Delta H_{rxn,298} = -10 \text{ kJ mol}^{-1} \quad (3)$$

The calculated reaction enthalpies clearly point to nitrosation of the phenol cation radical with neutral methyl nitrite (eq 3) as the only thermochemically possible reaction leading to $\mathbf{8}^{+\bullet}$. Note also that formation of the less stable *syn*-phenyl nitrite ion $\mathbf{9}^{+\bullet}$ was endothermic (eq 4) and should not compete with the exothermic formation of $\mathbf{8}^{+\bullet}$ (eq 3) in thermal collisions. The formation of ion $\mathbf{8}^{+\bullet}$ by reaction 3 is also perfectly compatible with the result of the ion−molecule reaction of mass-selected $C_6H_5OH^{+\bullet}$ with *tert*-butyl nitrite (vide supra). In this case, the 3−5 eV kinetic energy of the ion could be sufficient to drive even the mildly endothermic formation of the less stable *syn*-conformer $\mathbf{9}^{+\bullet}$ (eq 4).

$$C_6H_5OH^{+\bullet} + CH_3ONO \rightarrow \textit{syn}\text{-}C_6H_5ONO^{+\bullet} + CH_3OH \quad \Delta H_{rxn,298} = 12 \text{ kJ mol}^{-1} \quad (4)$$

In contrast, nitrosations of neutral phenol with $CH_3O(NO)_2^+$ to yield $\mathbf{8}^{+\bullet}$ (reactions 1 and 2) were too endothermic to proceed at reasonable rates under thermal conditions.

Are reactions 1 and 2 disfavored by the formation of radical products? To answer this question we calculated the reaction enthalpy for simple NO^+ transfer onto phenol without a hydrogen atom rearrangement to yield protonated phenyl nitrite $\mathbf{17}^+$. Equation 5 shows that simple nitrosation of phenol with $CH_3O(NO)_2^+$ was substantially endothermic and therefore inefficient in the gas phase.

$$C_6H_5OH + CH_3O(NO)_2^+ \rightarrow C_6H_5O(H)NO^+ + \textit{syn}\text{-}CH_3ONO \quad \Delta H_{rxn,298} = 106 \text{ kJ mol}^{-1} \quad (5)$$

In contrast, nitrosation of phenol with bare NO^+ to form $\mathbf{17}^+$ was calculated to be exothermic (eq 6) and therefore possible under the conditions of gas-phase ion−molecule reactions.

$$C_6H_5OH + NO^+ \rightarrow C_6H_5O(H)NO^+ \quad \Delta H_{rxn,298} = -25 \text{ kJ mol}^{-1} \quad (6)$$

$$C_6H_5O(H)NO^+ + \textit{syn}\text{-}CH_3ONO \rightarrow \textit{anti}\text{-}C_6H_5ONO + CH_3O(H){-}NO^+ \quad \Delta H_{rxn,298} = 52 \text{ kJ mol}^{-1} \quad (7)$$

Moreover, a further reaction of adduct $\mathbf{17}^+$ by proton transfer to CH_3ONO was endothermic (eq 7) and therefore inefficient. Once formed by reaction 6, ion $\mathbf{17}^+$ should be stable under the reaction conditions. However, reaction 6 must compete with charge transfer between NO^+ and C_6H_5OH which is exothermic by 75 kJ mol^{-1} (from the corresponding adiabatic ionization energies[5] of phenol and NO, 81 kJ mol^{-1} from B3-PMP2 calculations) and evidently faster than the addition (Figure 5a).

Dissociations of $C_6H_5NO_2H$ Cations and Isomers. $[C_6,H_5,N,O_2]^{+\bullet}$ cation-radicals were also produced by CAD loss of H from protonated nitrobenzene $\mathbf{15}^+$ that competed with eliminations of OH, HONO, and NO.[9] The hydrogen atom eliminated originated entirely from the ring positions as established from the CAD spectra of $C_6H_5NO_2D^+$ ($\mathbf{15a}^+$) that showed a clean loss of H, and $C_6D_5NO_2H^+$ ($\mathbf{15b}^+$) that showed loss of D only. The ring hydrogen atoms were distinguished using specifically labeled nitrobenzene ions *o*-*d*-$C_6H_4NO_2H^+$ ($\mathbf{15c}^+$) *m*-*d*-$C_6H_4NO_2H^+$ ($\mathbf{15d}^+$), and *p*-*d*-$C_6H_4NO_2H^+$($\mathbf{15e}^+$) that were prepared by $CH_3C{=}NH^+/CH_3CN$ chemical ionization of the corresponding labeled nitrobenzenes.[9] The relative intensities of $[MH-H]^+$ and $[MH-D]^+$ ions were fitted in homogeneous mass balance equations (eqs 8−10) that were solved to yield the fractions for the loss of H from the *ortho*, *meta*, and *para* positions denoted by [ortho], [meta], and [para], respectively. The best fit was obtained by considering an average isotope effect $k_H/k_D = 2.00$.

$$\frac{k_D/k_H[\text{ortho}]}{[\text{ortho}] + 2[\text{meta}] + [\text{para}]} = \frac{[\mathbf{15c}{-}D]}{[\mathbf{15c}{-}H]} = \frac{0.029}{0.971} \quad (8)$$

$$\frac{k_D/k_H[\text{meta}]}{2[\text{ortho}] + [\text{meta}] + [\text{para}]} = \frac{[\mathbf{15d}{-}D]}{[\mathbf{15d}{-}H]} = \frac{0.176}{0.824} \quad (9)$$

$$\frac{k_D/k_H[\text{para}]}{2[\text{ortho}] + 2[\text{meta}]} = \frac{[\mathbf{15c}{-}D]}{[\mathbf{15c}{-}H]} = \frac{0.167}{0.833} \quad (10)$$

The obtained fractions, [ortho] = 0.06, [meta] = 0.29, [para] = 0.30, when adjusted for the fact that there are two equivalent *ortho* and *meta* positions, gave the H-loss from the *ortho*, *meta*, and *para* positions as 12, 58, and 30%, respectively. The fractions did not depend on the ion transmittance (*T*) used in the CAD spectra and were practically the same for dissociations at 70% and 50% *T*.

An interesting feature of these dissociations was that they competed with the lowest-energy dissociations of $\mathbf{15}^+$, e.g., elimination of NO, loss of OH, and elimination of HONO that required 34, 264, and 279 kJ mol^{-1} at the respective B3-MP2 thermochemical thresholds. The thermochemical data (Table 2) show that direct loss of ring hydrogen atoms from $C_6H_5NO_2H^+$ required extreme energies, e.g., 474 kJ mol^{-1} to form $\mathbf{4}^{+\bullet}$, which should prevent it from competing with the lower energy dissociations. A different mechanism was therefore sought to explain the loss of ring hydrogen atoms from $C_6H_5NO_2H^+$. An energetically plausible mechanism should allow the hydrogen loss to form a stable $[C_6H_5NO_2]^{+\bullet}$ isomer such that the stability of the product ion would compensate for the C−H bond dissociation energy. Of necessity, this would require a rearrangement in the protonated nitro group to avoid the formation of the high-energy isomers $\mathbf{2}^{+\bullet}$− $\mathbf{4}^{+\bullet}$.

Plausible mechanisms for low-energy loss of ring hydrogen atoms from $\mathbf{15}^+$ are shown in Schemes 3 and 4. The optimized geometries of the $[C_6,H_6,N,O_2]^+$ cations that are discussed in the text are summarized in Figure 11. The mechanism in Scheme 3 assumes a rearrangement of $\mathbf{15}^+$ to protonated phenyl nitrite $\mathbf{16}^+$ which is slightly more stable than $\mathbf{15}^+$. The transition state for the rearrangement was sought by detailed mapping by B3LYP/6-31+G(d,p) calculations of the relevant parts of the potential energy surface that interconnected ions $\mathbf{15}^+$ and $\mathbf{16}^+$. The potential energy surface showed two valleys corresponding to continuously endothermic dissociations of the C−N bond in $\mathbf{15}^+$ and C−O bond in $\mathbf{16}^+$ to form an ion molecule complex of $C_6H_5^+$ with *anti*-HONO. Attempts to cross the ridge separating the valleys resulted in an increased potential energy and did not yield a saddle point at C−N and C−O distances

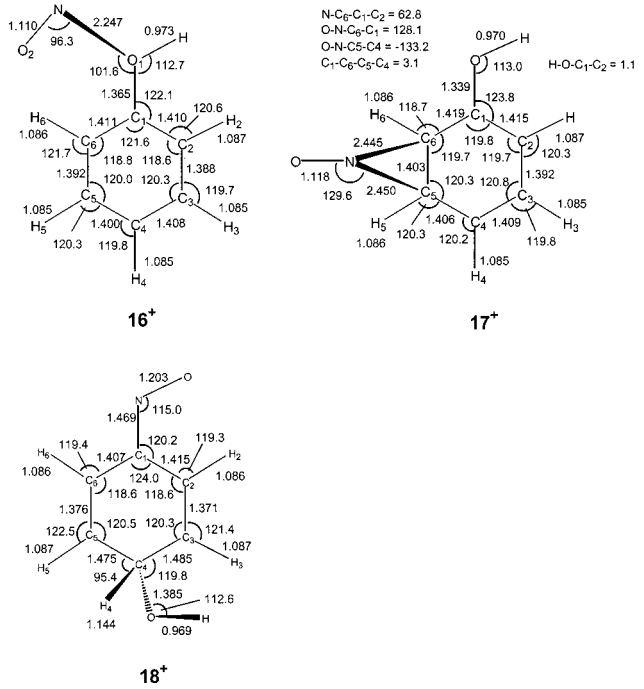

Figure 11. B3LYP/6-31+G(d,p) optimized structures of $[C_6,H_6,N,O_2]^+$ cations. Bond lengths in angstroms, bond and dihedral angles in degrees.

SCHEME 3

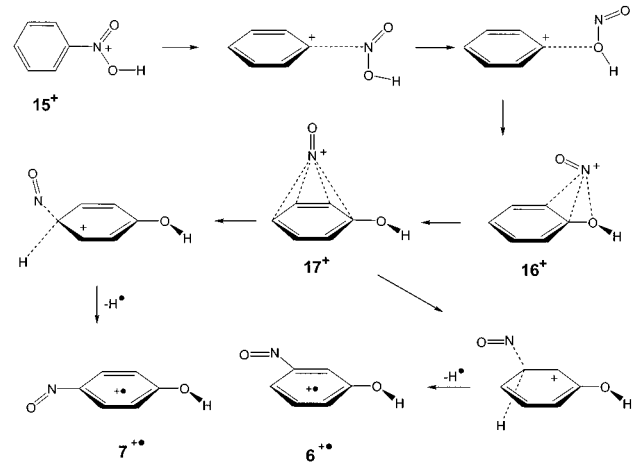

that would indicate a cyclic transition state with partially formed C−N and C−O bonds. We conclude that at the present level of theory structures $\mathbf{15}^+$ and $\mathbf{16}^+$ are not connected by a cyclic transition state that would correspond to $C_6H_5^+$ migration between the N and O atoms in $\mathbf{15}^+$. The isomerization likely proceeds in a $C_6H_5^+\cdots$HONO ion−molecule complex, and its activation energy is bound from above by the dissociation energy of the C−N bond in $\mathbf{15}^+$ (279 kJ mol^{-1}).

Following isomerization to $\mathbf{16}^+$, the NO group can migrate further to form ion $\mathbf{17}^+$ which is 69 kJ mol^{-1} more stable than $\mathbf{15}^+$ and represents the global minimum of the $C_6H_6NO_2^+$ isomers. Ion $\mathbf{17}^+$ can be viewed as a π-complex of NO^+ with phenol, as deduced from its structure (Figure 11) and the calculated charge distributions that showed 70% of positive charge residing in the NO moiety. Likewise, ion $\mathbf{16}^+$ (Figure 11) can be viewed as a σ-complex of NO^+ with the OH group in phenol, as indicated by the charge distributions that showed 70% of positive charge in the NO group. The activation barrier for the $\mathbf{16}^+ \rightarrow \mathbf{17}^+$ isomerization was not studied, but because of the relatively weak bonding of NO^+ and comparable energies of $\mathbf{16}^+$ and $\mathbf{17}^+$ it can be reasonably expected to be small. Loss of H from $\mathbf{17}^+$ requires electrophilic attack by the NO^+ group at one of the ring positions followed by homolytic C−H bond cleavage. The latter cleavage is substantially endothermic even for the formation of the most stable ion $\mathbf{7}^{+\bullet}$ (286 kJ mol^{-1}, Table 3). This is to be compared with loss of NO from $\mathbf{17}^+$ that requires only 112 kJ mol^{-1} and represents a simple bond cleavage that should not require an activation barrier above the thermochemical threshold. Hence, Scheme 3 does not explain satisfactorily how the loss of H can compete with the loss of NO.

An alternative mechanism assumes migration onto the ring of the NO_2H hydroxyl group followed by a ring-walk[39] to the *meta* and *para* positions (Scheme 4). The intermediates can eliminate competitively OH or H to form $C_6H_5NO^{+\bullet}$ or the nitrosophenol isomers $\mathbf{5}^{+\bullet}-\mathbf{7}^{+\bullet}$, respectively. Table 3 shows that these dissociations are comparable energetically, with the formation of $\mathbf{7}^{+\bullet}$ having the lowest threshold energy. The relative energies of the corresponding Wheland intermediates were not prohibitively high, e.g., $\mathbf{18}^+$ which was 141 kJ mol^{-1} above $\mathbf{15}^+$ and thus below the dissociation thresholds (Table 3). The kinetics for loss of H according to Scheme 4 depends on the energy barriers for OH migrations. The kinetic bottleneck is likely to be in the OH group migration to the *ortho*-position that formally requires a four-membered transition state. The fact that competitive eliminations of *ortho*-, *meta*, and *para* hydrogen atoms were observed experimentally suggests that the ring-walk of the OH group was not the rate-determining step. If it were, the *meta* and *para*-H eliminations would be increasingly disfavored against the *ortho*-H elimination, contrary to experiment. Likewise, isomerization by migration of ring hydrogen atoms would at the limit result in a stochastic (40%) loss of the *ortho*-hydrogen atoms contrary to experiment. We conclude that the mechanisms in Scheme 4 are consistent with experiment and calculated energies.

Formation of Neutral $[C_6H_5NO_2]$ Isomers. The ions generated by electron ionization, dissociative ionization, and ion−molecule reactions were used to generate transient neutral molecules by femtosecond collisional electron transfer. The intensities of $\mathbf{3}^{+\bullet}$ and $\mathbf{4}^{+\bullet}$ from the CI-CAD/CAD experiments were too low to be used for NR measurements. The intermediates were characterized by neutralization−reionization (NR) mass spectra that also provided an additional means of precursor ion distinction. A NR mass spectrum of $\mathbf{1}^{+\bullet}$ was reported previously[9] and is shown for reference in Figure 12a. For reasons discussed below, ions $\mathbf{1}^{+\bullet}$ were also generated by charge exchange (CE) ionization with $CS_2^{+\bullet}$ that is close to thermoneutral, IE(CS_2) − IE(**1**) = 10.07 − 9.94 = 0.13 eV (12.5 kJ mol^{-1}), and should form ion $\mathbf{1}^{+\bullet}$ in its ground electronic state. Furthermore, under the conditions of CE ionization ions $\mathbf{1}^{+\bullet}$ are likely to be thermalized by collisions with the reagent gas at the ion source temperature (523−573 K). The NR mass spectrum of $\mathbf{1}^{+\bullet}$ by CE ionization was identical with that from electron ionization at 70 eV. In contrast, collisional activation of intermediate **1** resulted in an efficient decrease of the relative intensity of the $\mathbf{1}^{+\bullet}$ survivor ion. For example, at 50% transmittance of the neutral beam due to collisions, the relative abundance of $\mathbf{1}^{+\bullet}$ dropped to 60% of the initial value, indicating >80% dissociation efficiency upon collisional activation (Figure 12c). These data were used to interpret the NR mass spectrum of the $[C_6H_5NO_2]^{+\bullet}$ ion from *o*-nitrobenzoic acid (Figure 12b). This spectrum showed fragment ions that were identical with those in the NR spectrum of $\mathbf{1}^{+\bullet}$ but lacked the survivor ion. From the strong dependence of the survivor ion intensity on internal energy we concluded that the ion from *o*-nitrobenzoic

TABLE 3: Dissociation and Isomerization Energies of Protonated Nitrobenzene Isomers

	energy[a]					
reaction	B3LYP/ 6-31+G(d,p)	B3LYP/ 6-311+G(2df,p)	PMP2/ 6-311+G(2df,p)	ROMP2/ 6-311+G(2df,p)	B3-PMP2	B3-ROMP2
$\mathbf{15}^+ \rightarrow C_6H_5^+ + \textit{anti}$-HONO	262	259	298	*b*	279	*b*
$\mathbf{15}^+ \rightarrow C_6H_5^+ + \textit{syn}$-HONO	264	261	300	*b*	281	*b*
$\mathbf{15}^+ \rightarrow C_6H_5OH^{+\bullet} + NO^\bullet$	20	19	66 (68)[c]	48	43	34
$\mathbf{15}^+ \rightarrow C_6H_5OH + NO^+$	179	159	95 (93)[c]	*b*	127	*b*
$\mathbf{15}^+ \rightarrow C_6H_5NO^{+\bullet} + OH^\bullet$	227	229	294 (296)[c]	299	261	264
$\mathbf{15}^+ \rightarrow \mathbf{4}^{+\bullet} + H^\bullet$	480	475	485 (489)[c]	474	480	474
$\mathbf{15}^+ \rightarrow \mathbf{5}^{+\bullet} + H^\bullet$	236	230	265	260	248	245
$\mathbf{15}^+ \rightarrow \mathbf{6}^{+\bullet} + H^\bullet$	252	244	273	256	258	250
$\mathbf{15}^+ \rightarrow \mathbf{7}^{+\bullet} + H^\bullet$	207	200	234	235	217	217
$\mathbf{15}^+ \rightarrow \mathbf{16}^+$	−13	−20	−42 (−44)[c]	*b*	−31	*b*
$\mathbf{15}^+ \rightarrow \mathbf{17}^+$	−47	−53	−85 (−88)[c]	*b*	−69	*b*
$\mathbf{15}^+ \rightarrow \mathbf{18}^+$	128	132	150	*b*	141	*b*
$\mathbf{15}^+ \rightarrow \mathbf{19}^+$	86	88	110 (109)[c]	*b*	99	*b*
$\mathbf{17}^+ \rightarrow \mathbf{9} + H^+$	833	840 (844)[c]	847 (854)[c]	*b*	844 (849)[c]	*b*
$\mathbf{19}^+ \rightarrow \mathbf{9} + H^+$	734	733 (736)[c]	695 (700)*c*	*b*	714 (718)[c]	*b*

In units of kJ mol^{-1} at 298 K. [b] Closed shell products. [c] From single-point energies calculated with the 6-311+G(3df,2p) basis set.

SCHEME 4

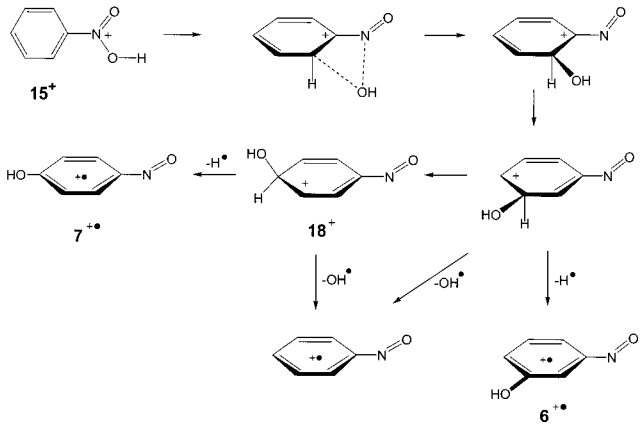

acid had structure $\mathbf{1}^{+\bullet}$ but was formed with a high internal energy that drove dissociations in NRMS. This conclusion is consistent with the CAD spectra that showed very similar dissociations for the ions in question (vide supra).

It is also pertinent to note that collisional activation of neutral **1** did not result in substantially enhanced relative intensities of ions characteristic of phenyl nitrite ($\mathbf{8}^{+\bullet}$), e.g., $C_6H_5O^+$ at *m*/*z* 93 and $C_5H_5^+$ at *m*/*z* 65 (Figure 13a). This indicated that on the 5.3 μs time scale, excited **1** did not isomerize to **8** to an extent that would be detectable by the NR mass spectrum.

Entirely different NR mass spectra were obtained for ions $\mathbf{7}^{+\bullet}$, $\mathbf{8}^{+\bullet}$, and the ion from dissociative ionization of *o*-nitroacetophenone. NR of $\mathbf{7}^{+\bullet}$ furnished an abundant survivor ion in keeping with the substantial stability of both neutral **7** and ion $\mathbf{7}^{+\bullet}$ (Figure 13b). NR of $\mathbf{8}^{+\bullet}$ showed a very weak survivor ion and fragmentations compatible with the structure of phenyl nitrite, e.g., loss of NO (*m*/*z* 93), absence of loss of OH (*m*/*z* 106), and weak loss of NO_2 (*m*/*z* 77, Figure 13a). The low stability of survivor ion $\mathbf{8}^{+\bullet}$ is probably due to Franck−Condon effects on both vertical electron attachment in $\mathbf{8}^{+\bullet}$ and subsequent collisional ionization of **8**. The respective Franck−Condon energies were calculated as 57 and 91 kJ mol^{-1} which, when combined, were sufficient for driving the dissociation of reionized $\mathbf{8}^{+\bullet}$ to $C_6H_5O^+$ and NO that required 122 kJ mol^{-1}at 0 K. (Table 2).

The NR mass spectrum of the $[C_6H_5NO_2]^{+\bullet}$ ion from *o*-acetophenone (Figure 13c) showed a moderate survivor ion and dissociations by loss of OH (*m*/*z* 106), and NO (*m*/*z* 93),

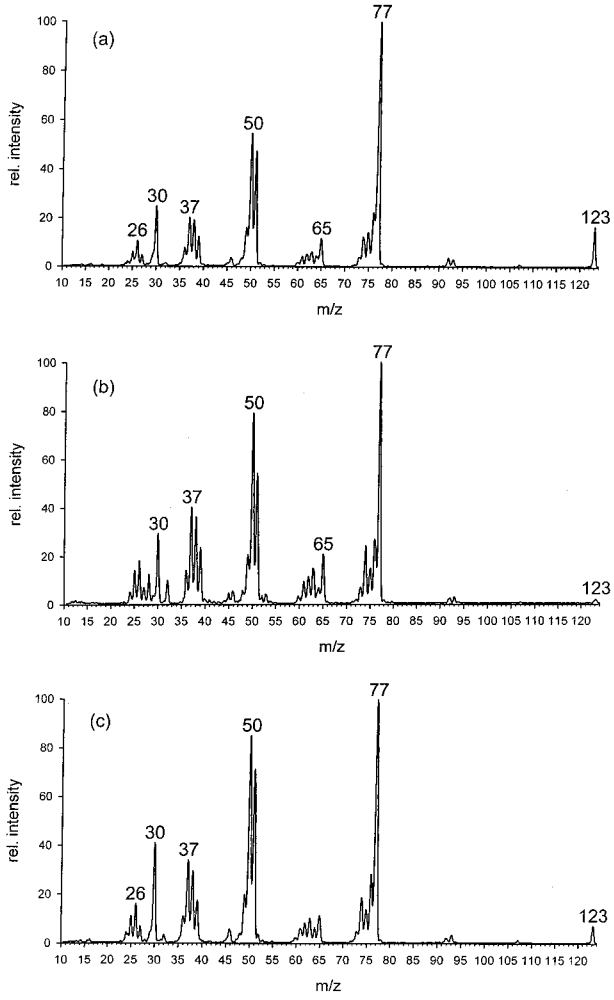

Figure 12. Neutralization (CH_3SSCH_3, 70% transmittance)−reionization (O_2, 70% transmittance) mass spectra of (a) $\mathbf{1}^{+\bullet}$, (b) *m*/*z* 123 ion from *o*-nitrobenzoic acid. (c) Neutralization (CH_3SSCH_3, 70% transmittance)−collisional activation (He, 70% transmittance)−reionization (O_2, 70% transmittance) mass spectrum of $\mathbf{1}^{+\bullet}$.

while loss of NO_2 to give *m*/*z* 77 was negligible. The absence of $C_6H_5^+$ strongly argues against a monosubstituted benzene structure for the precursor ion and neutral intermediate. An *ortho*-ylid-ion structure ($\mathbf{2}^{+\bullet}$) could be expected to eliminate HONO which was excluded by the weak $C_6H_4^{+\bullet}$ fragment at *m*/*z* 76. Note also that ion $\mathbf{2}^{+\bullet}$ was likely to undergo facile

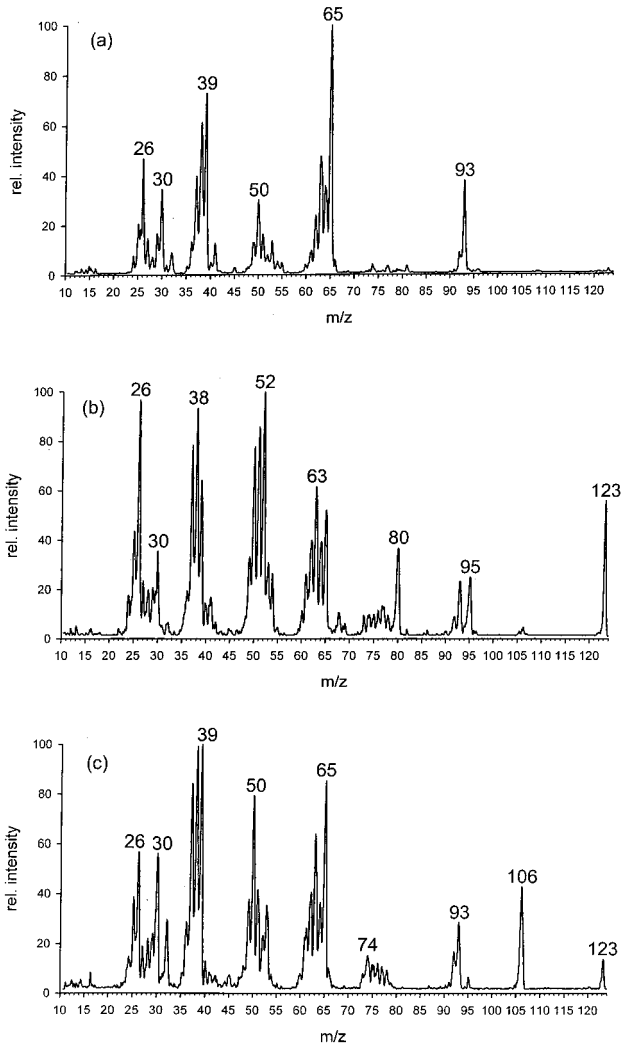

Figure 13. Neutralization (CH_3SSCH_3, 70% transmittance)−reionization (O_2, 70% transmittance) mass spectra of (a) phenyl nitrite cation-radical $\mathbf{8}^{+\bullet}$, (b) *p*-nitrosophenol cation-radical $\mathbf{7}^{+\bullet}$, (c) *m*/*z* 123 ion from *o*-nitroacetophenone.

SCHEME 5

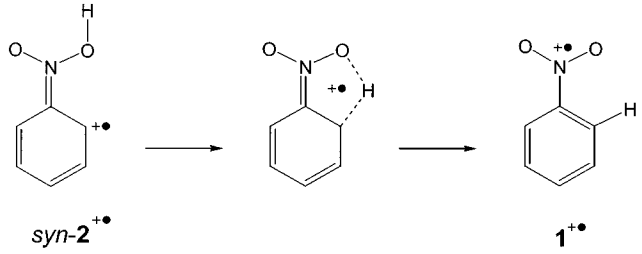

isomerization to $\mathbf{1}^{+\bullet}$, as observed for the ion generated by loss of NO_2 from protonated *o*-dinitrobenzene (Scheme 5). The transition state for $\mathbf{2}^{+\bullet} \rightarrow \mathbf{1}^{+\bullet}$ was only 70 kJ mol^{-1} above $\mathbf{2}^{+\bullet}$, which was well below the ion dissociation thresholds (Table 2). However, fragment ions that would indicate the presence of $\mathbf{1}^{+\bullet}$ were unimportant in the NR mass spectrum of the $[C_6H_5NO_2]^{+\bullet}$ ion from *o*-acetophenone (Figure 13c). The observed competitive losses of OH and NO were in keeping with the structures of *o*-nitrosophenol ($\mathbf{5}^{+\bullet}$), *o*-benzoquinone monooxime ($\mathbf{10}^{+\bullet}$), or *o*-benzoquinone mononitrone ($\mathbf{11}^{+\bullet}$) which were all stable, low-energy ions (Table 1) that also had stable neutral counterparts (Table 4). Unfortunately, the corresponding neutral molecules are unknown and, very likely, highly reactive, so that reference spectra could not be obtained for comparison. One

TABLE 4: Relative Energies of Neutral $C_6H_5NO_2$ Isomers

	relative energy[a]			
species	B3LYP/ 6-31+G(d,p)	B3LYP/ 6-311+G-(2df,p)	PMP2/ 6-311+G-(2df,p)	B3-PMP2
1	0	0	0	0
(^1A) *syn*-**2**	330	332	370 (368)[b]	351
($^3A''$) *syn*-**2**	266	267	346 (345)[b]	307
(^1A) *anti*-**2**	335	337	372	355
($^3A''$) *anti*-**2**	270	271	349	310
(^1A) *syn*-**3**	324	324	341 (339)[b]	332
($^3A''$) *syn*-**3**	265	267	350	308
(^1A) *anti*-**3**	322			
($^3A''$) *anti*-**3**	265	266	350	303
(^1A) **4**	351	352	406 (405)[b]	379
($^3A''$) **4**	263	265	340	303
5	−64	−59	−39	−49
6	−33	−30	−21	−25
7	−43	−41	−25	−33
8	5	5	20	12
9	11	11	22	16
10	−51	−47	−18	−32
11	−38	−35	−16	−26
13	96	96	109	103
syn-**19**	−14	−13	14	0.4
anti-**19**	−45	−41	−15	−28

[a] In units of kJ mol^{-1} at 0 K. [b] From single-point calculations with the 6-311+G(3df,2p) basis set.

SCHEME 6

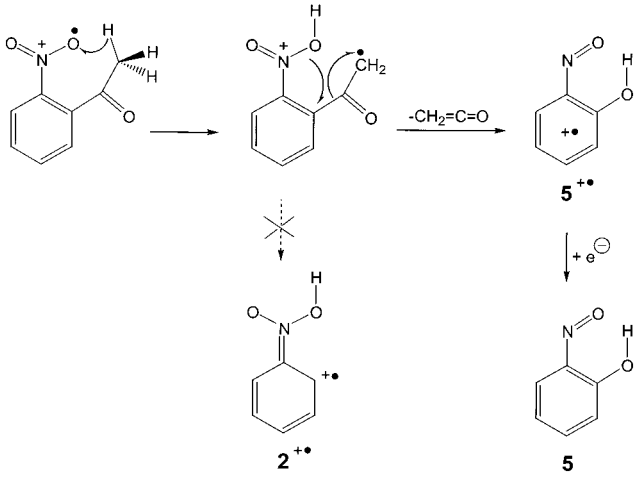

can presume facile interconversion of ions $\mathbf{5}^{+\bullet}$, $\mathbf{10}^{+\bullet}$, and $\mathbf{11}^{+\bullet}$ by proton transfer through five- or six-membered cyclic transition states that could result in dissociation by loss of OH or NO from either structure. This, and the fact that the ions are formed from the *o*-acetophenone precursor by a hydrogen rearrangement, would favor the most stable structure $\mathbf{5}^{+\bullet}$ for the isomer in question. The formation of ion $\mathbf{5}^{+\bullet}$ is tentatively depicted in Scheme 6.

Ionization Energies. The potential energy surfaces of the neutral $[C_6,H_5,N,O_2]$ isomers and the corresponding cation-radicals are connected by ionization energies that were calculated for the entire set of structures (Table 6). Comparison with experimental data was possible only for **1** where the B3-MP2 adiabatic ionization energies showed excellent agreement with the tabulated value (9.94 ± 0.08 eV).[5] Carbenes **2**−**4** had low ionization energies which should make them readily oxidizable if formed as reactive intermediates. The ionization energies of nitrosophenols **5**−**7** were lower than that of phenol (8.49 eV)[5] and indicated that the nitroso group is a weak electron acceptor that increases the HOMO energy by participation of dipolar

TABLE 5: Dissociation Energies of Neutral $C_6H_5NO_2$ Isomers

reaction	dissociation energy[a] B3LYP/ 6-31+G(d,p)	B3LYP/ 6-311+G(2df,p)	PMP2/ 6-311+G(2df,p)	B3-PMP2
1 → $C_6H_5^{\bullet}$ + $NO_2^{\bullet}$	282	277	325	301 (305)[c](307)[b,c]
1 → $C_6H_5O^{\bullet}$ + $NO^{\bullet}$	67	67	117 (93)[d]	92 (93)[b](80)[b,d]
(^1A) *syn*-**2** → ($^1A_1$) *o*-C_6H_4 + *anti*-HONO	3	−5	−34	−19
($^3A''$) *syn*-**2** → ($^3B_2$) *o*-C_6H_4 + *anti*-HONO	192	190	170	180
(^1A) *syn*-**3** → ($^1A_1$) *m*-C_6H_4 + *anti*-HONO	57	53	50	51
($^3A''$) *syn*-**3** → ($^3B_2$) *m*-C_6H_4 + *anti*-HONO	175	172	182	177
(^1A) **4** → (^1A_g) *p*-C_6H_4 + *anti*-HONO	131	129	−21	54
($^3A''$) **4** → ($^3B_{1u}$) *p*-C_6H_4 + *anti*-HONO	172	169	152	160
8 → $C_6H_5O^{\bullet}$ + $NO^{\bullet}$	62	62	98 (73)[d]	80 (68) (68)[b,d]

[a] In units of kJ mol^{-1} at 0 K. [b] From single-point calculations with the 6-311+G(3df,2p) basis set. [c] At 298 K. [d] From ROMP2/6-311+G(2df,p) single-point calculations.

TABLE 6: Ionization Energies of $C_6H_5NO_2$ Isomers

species	ionization energy[a] B3LYP/ 6-31+G(d,p)	B3LYP/ 6-311+G(2df,p)	PMP2/ 6-311+G(2df,p)	ROMP2/ 6-311+G(2df,p)	B3-PMP2	B3-ROMP2
1	9.73	9.76	10.00	9.94 (9.94)[b]	9.88	9.85
(^1A) *syn*-**2**	6.76	6.73	6.67	6.61	6.70	6.67
($^3A''$) *syn*-**2**	7.42	7.40	6.92	6.86	7.16	7.13
(^1A) *anti*-**2**	6.74	6.72	6.68		6.70	
($^3A''$) *anti*-**2**	7.41	7.40	6.93		7.16	
(^1A) *syn*-**3**	6.83	6.83	7.01	6.88	6.92	6.85
($^3A''$) *syn*-**3**	7.38	7.36	6.84	6.71	7.10	7.03
($^3A''$) *anti*-**3**	7.38	7.36	6.84		7.10	
(^1A) **4**	6.46	6.44	6.23	6.11	6.33	6.27
($^3A''$) **4**	7.35	7.33	6.90	6.78	7.12	7.06
5	8.28	8.21	8.62	8.56	8.42	8.39
6	8.11	8.06	8.51	8.34	8.28	8.20
7	7.77	7.71	8.15	8.16	7.93	7.94
8	8.21	8.15 (8.14)[b]	8.24 (8.25)[b]	8.12 (8.14)[b]	8.19 (8.20)[b]	8.14 (8.14)[b]
9	8.36	8.30	8.45	8.32	8.37	8.31
10	8.80	8.81	9.12	9.02	8.97	8.91
11	8.47	8.49	8.80	8.52	8.65	8.50
13	7.73	7.73	8.16	8.03	7.94	7.88

[a] Adiabatic ionization energies in units of electronvolts. [b] From single-point calculations with the 6-311+G(3df,2p) basis set.

canonical structures of the $^-O-N{=}C_6H_4{=}OH^+$ type. The ionization energies of **8**−**13** were unexceptional.

Concerning collisional electron transfer, the IE_a values for **5**, **10**, and **11** (Table 6) allow cation-radicals $\mathbf{5}^{+\bullet}$, $\mathbf{10}^{+\bullet}$, and $\mathbf{11}^{+\bullet}$ to undergo exothermic electron transfer from CH_3SSCH_3, but not from NO, in keeping with the observed ion−molecule reactions (vide supra). Hence, on the basis of the present experimental data these structures remain unresolved. Charge-transfer reactions with thermal electron donors[40] could possibly distinguish isomers $\mathbf{5}^{+\bullet}$ and $\mathbf{11}^{+\bullet}$ from $\mathbf{10}^{+\bullet}$, although distinction of $\mathbf{5}^{+\bullet}$ and $\mathbf{11}^{+\bullet}$ whose recombination energies differ by 0.1 eV would be difficult (Table 6).

Neutral Structures and Energies. Ions $\mathbf{1}^{+\bullet}$−$\mathbf{14}^{+\bullet}$ have stable neutral counterparts that were investigated by calculations. The corresponding optimized structures are given in Figure 14, the relative energies are summarized in Table 4. An interesting feature of structures **2**−**4** is that the neutral molecules can exist as singlet or triplet electronic states that differ in geometry parameters. Structures **2** and **4** can be viewed as nitronic acids derived from 2,4-cyclohexadienone-6-carbene, and 2,5-cyclohexadienone-4-carbene, respectively, whereas structure **3** corresponds to a nitronic acid of 2,4,5-cyclohexatrienone (Scheme 7). The triplet meta isomers ($^3A''$) *syn*- and *anti*-**3** can be depicted as biradicals on the basis of the calculated spin densities that were 0.50, 0.50, and 1.19 at the N, O, and carbene C-3 atom, respectively. The triplet structures were consistently more stable than the singlets, although the energy differences depended on the computational method used. B3LYP consistently favored the triplet states whereas MP2 gave much smaller singlet−triplet gaps. The B3-PMP2 calculations gave the singlet−triplet gaps as 44, 24, and 76 kJ mol^{-1} for *syn*-**2**, *syn*-**3**, and *syn*-**4**, respectively. In general, however, neutral carbenes **2**−**4** were substantially less stable than **1** and could exist only thanks to energy barriers to exothermic isomerization to **1**. A similar trend was obtained for dissociation energies of **2**−**4** (Table 5). Singlet carbenes **2** and **4** were only weakly bound with respect to dissociation by loss of *anti*-HONO to form the corresponding singlet benzynes (Table 5). The dissociation thresholds for HONO loss from the more stable triplet states of **2** and **4** were somewhat higher to make the carbenes kinetically stable. The meta carbenes (^1A) and ($^3A''$) *syn*-**3** were both substantially bound with respect to elimination of HONO (Table 5) and represent the best candidates for attempts at preparation in the gas phase.

Phenyl nitrite conformers **8** and **9** were slightly less stable than **1**, and their relative stabilities indicated that both conformers should be populated at equilibrium in the gas phase. We calculated the corresponding free energies for interconversion **8** → **9**, ΔG_T = 3.6 and 3.1 kJ mol^{-1} at 298 and 523 K, respectively, that indicated 19−33% of the *syn*-isomer at gas-phase equilibrium within this temperature range. The threshold energy for dissociation to $C_6H_5O^{\bullet}$ and NO of the more stable conformer **8** was very low (68 kJ mol^{-1} at 0 K, Table 5) which explains the low stability and elusive character of phenyl nitrite.

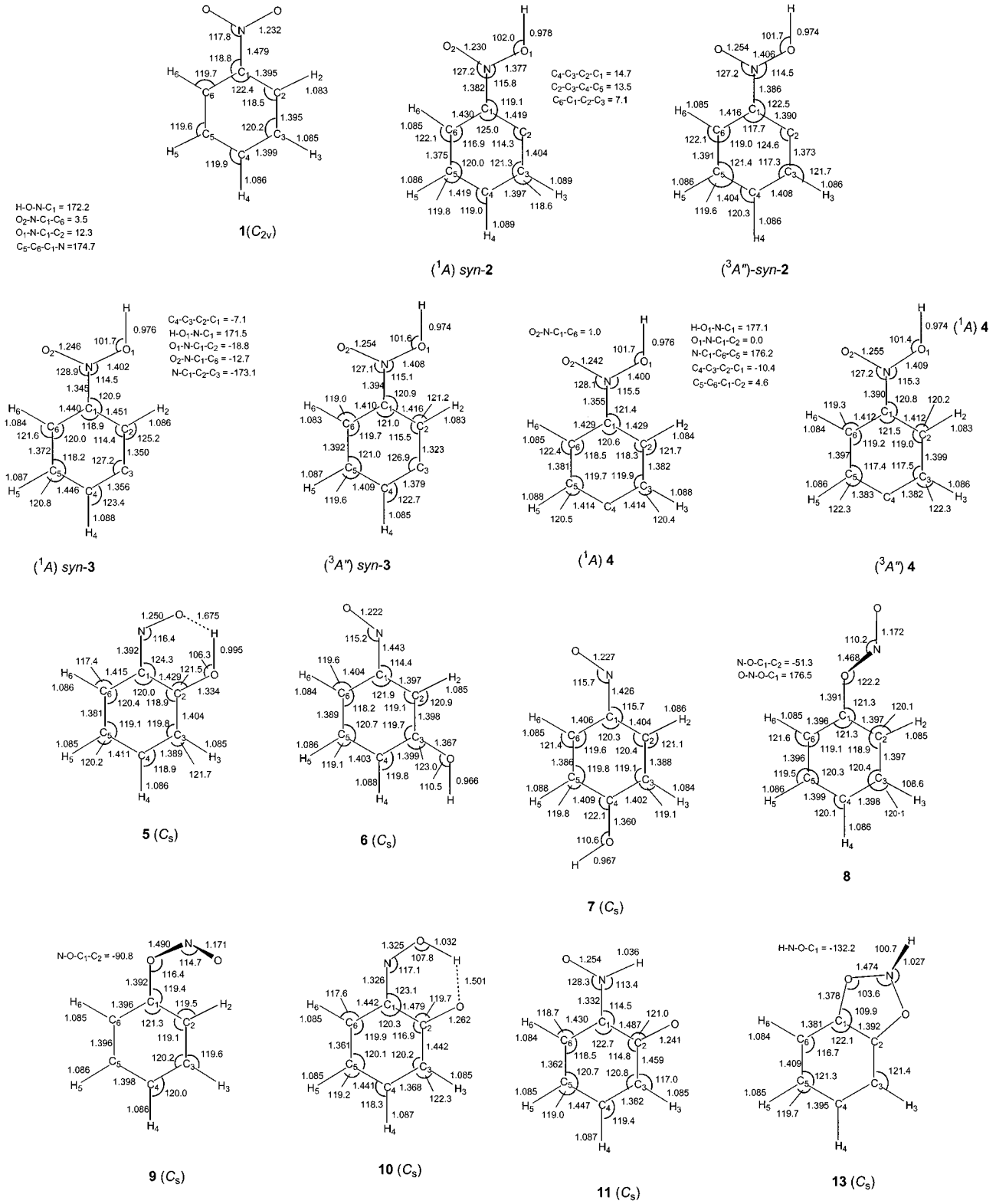

Figure 14. B3LYP/6-31+G(d,p) optimized structures of $[C_6,H_5,N,O_2]$ neutral molecules. Bond lengths in angstroms, bond and dihedral angles in degrees.

The cyclic isomer **13** was substantially less stable than **1**, indicating that condensation of the 1,3-dioxa-2-azolidine and benzene rings resulted in a high-energy structure. The isomeric benzo[*d*]-1,2-dioxa-3-azolidine (**12**) was not a stable structure. Upon geometry optimization, **12** underwent ring opening to yield a rotamer of *o*-benzoquinone mononitrone. The nitrosophenol isomers **5**−**7**, *o*-benzoquinone mononitrone **10** and mono oxime **11**, and *p*-benzoquinone mono oxime anti-**19** were all thermodynamically more stable than **1**. The fact that these isomers are unknown as stable, isolable compounds must be due to their high reactivity in the condensed phase. This is consistent with the high reactivity and hence low stability of *o*-benzoquinone,[41] quinonoids,[42] and sterically unhindered nitrones.[43] It is interesting to note that **7** and **19** are tautomers that can isomerize by acid−base-catalyzed proton transfer.[42] The very similar relative energies of **7** and **20** indicate that both structures must be

SCHEME 7

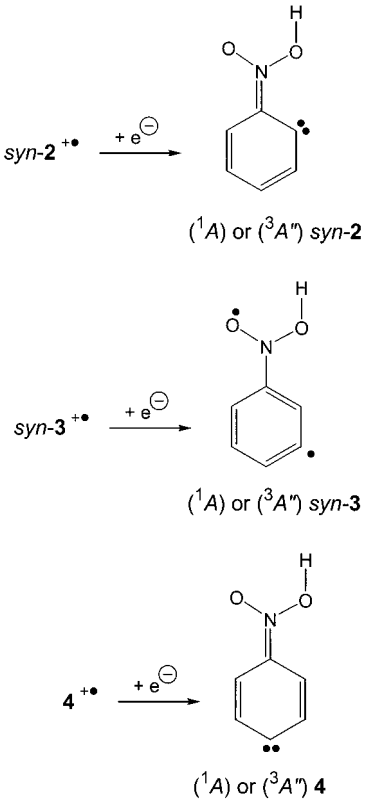

populated at an equilibrium. The B3-PMP2 calculated free energies for **19** → **7** $\Delta G_T = -4.4$ and -4.2 kJ mol^{-1} at 298 and 523 K, respectively, indicated 14−28% of **19** at gas-phase equilibrium within this temperature range.

Conclusions

Five distinct isomers of nitrobenzene cation-radical (**1**$^{+\bullet}$) were generated in the gas phase and investigated by collisionally activated dissociations, ion−molecule reactions, and neutralization−reionization mass spectrometry. Ylid-ions **3**$^{+\bullet}$ and **4**$^{+\bullet}$ exist as stable species in the gas phase although they are thermodynamically less stable than **1**$^{+\bullet}$. The cation-radical of *p*-nitrosophenol (**7**$^{+\bullet}$) was stable in the gas phase. Ab initio calculations showed that **7**$^{+\bullet}$ represented the most stable ion isomer of the fourteen isomers investigated by theory. Collisional neutralization of phenyl nitrite cation-radical (**8**$^{+\bullet}$) was used to generate the hitherto elusive neutral **8** and characterize it by mass spectrometry. This allowed us to determine that, contrary to photoexcitation, collisional activation of neutral **1** did not result in isomerization to **8**.

Acknowledgment. The work performed at University of Washington was supported by the National Science Foundation (Grant CHE-9712570). The computations were performed at the Department of Chemistry Computer Facility that received generous funding from NSF (Grant CHE-9808182). We thank Dr. Martin Sadílek for technical assistance with CAD spectra measurements. The work performed at the University of Mons was supported by the Fonds National de la Recherche Scientifique (FNRS).

References and Notes

(1) (a) Mitscherlich, E. *Ann. Phys.* **1834**, *31*, 625. (b) Mitscherlich, E. *Ann. Pharm.* **1834**, *12*, 305.

(2) Ward, E. R. *Chem. Br.* **1979**, *15*, 297.

(3) Reichardt, C. *Solvents and Solvent Effects in Organic Chemistry*, 2nd ed.;VCH: Weinheim, 1990.

(4) (a) Urbanski, T. In *The Chemistry of the Nitro and Nitroso Groups*, Feuer, H., Ed.; Wiley-Interscience: New York, 1970; pp 64−73. (b) Olah, G. A.; Malhotra, R.; Narang, S. C. *Nitration, Methods and Mechanisms*; VCH Publishers: New York, 1989.

(5) *NIST Standard Reference Database No. 69*, February 2000 Release. http://webbook.nist.gov/chemistry

(6) Brill, T. B.; James, K. J. *Chem. Rev.* **1993**, *93*, 2667−2692.

(7) (a) Iyer, S.; Capellos, C. In *Advances in Chemical Reaction Dynamics*; Rentzepis, P. M., Capellos, C., Eds.; Reidel: Amsterdam, 1986; pp 405−414. (b) Kosmidis, C.; Ledingham, K. W. D.; Kilic, H. S.; McCanny, T.; Singhal, R. P.; Langley, A. J.; Shaikh, W. *J. Phys. Chem. A* **1997**, *101*, 2264−2270. (c) Berho, F.; Caralp, F.; Rayez, M.-T.; Lesclaux, R.; Ratajczak, E. *J. Phys. Chem. A* **1998**, *102*, 1−8.

(8) Glenewinkel-Meyer, T.; Crim, F. F. *J. Mol. Struct. (THEOCHEM)* **1995**, *337*, 209−224.

(9) (a) Polasek, M.; Turecek, F. *J. Am. Chem. Soc.* **2000**, *122*, 9511. (b) Polasek, M.; Turecek, F.; Gerbaux, P.; Flammang, R. Presented at the 48th Annual Conference of the American Society for Mass Spectrometry, Long Beach, CA, June 2000, Abstract No. 853.

(10) (a) Lavorato, D. J.; Terlouw, J. K.; Dargel, T. K.; Koch, W.; McGibbon, G. A.; Schwarz, H. *J. Am. Chem. Soc.* **1996**, *118*, 11898. (b) McGibbon, G. A.; Hrusak, J.; Lavorato, D.; Schwarz, H.; Terlouw, J. K. *Chem. Eur. J.* **1997**, *3*, 232. (c) McGibbon, G. A.; Heinemann, C.; Lavorato, D. J.; Schwarz, H. *Angew. Chem. Int. Ed. Engl.* **1997**, *36*, 1478. (d) Dargel, T. K.; Koch, W.; Lavorato, D. J.; McGibbon, G. A.; Terlouw, J. K.; Schwarz, H. *Int. J. Mass Spectrom.* **1999**, *185/186/187*, 925. (e) Lavorato, D. J.; Fell, L. M.; McGibbon, G. A.; Sen, S.; Terlouw, J. K.; Schwarz, H. *Int. J. Mass Spectrom.* **2000**, *195/166*, 71.

(11) (a) Beynon, J. H.; Saunders, R. A.; Williams, A. E. *Ind. Chim. Belge* **1964**, *29*, 311. (b) Bursey, M. M.; McLafferty, F. W. *J. Am. Chem. Soc.* **1966**, *88*, 5023. (c) Shapiro, R. H.; Serum, J. W. *Org. Mass Spectrom.* **1969**, *2*, 533. (d) Bursey, M. M. *Org. Mass Spectrom.* **1969**, *2*, 907. (e) Davis, B.; Williams, D. H. *Chem.* Commun. **1970**, 412. (f) Benoit, F.; Holmes, J. L. *Org. Mass Spectrom.* **1970**, *3*, 993−1007. (g) Benoit, F.; Holmes, J. L. *Chem. Commun.* **1970**, 1031. (h) Brown, P. *Org. Mass Spectrom.* **1970**, *3*, 1175. (i) Mamer, O. A.; Kominar, R. J.; Lossing, F. P. *Org. Mass Spectrom.* **1970**, *3*, 1411−1416. (j) Brown, P. *Org. Mass Spectrom.* **1970**, *4*, 533. (k) Engel, R.; Halpern, D.; Funk, B.-A. *Org. Mass Spectrom.* **1973**, *7*, 177. (l) Beynon, J. H.; Bertrand, M.; Cooks, R. G. *J. Am. Chem. Soc.* **1973**, *95*, 1739.

(12) (a) Danis, P. O.; Wesdemiotis, C.; McLafferty, F. W. *J. Am. Chem. Soc.* **1983**, *105*, 7454. (b) Burgers, P. C.; Holmes, J. L.; Mommers, A. A.; Terlouw, J. K. *Chem. Phys. Lett.* **1983**, *102*, 1.

(13) For most recent reviews see: (a) Zagorevskii, D.; Holmes, J. L. *Mass Spectrom. Rev.* **1999**, *18*, 87. (b) Schalley, C. A.; Hornung, G.; Schroder, D.; Schwarz, H. *Chem. Soc. Rev.* **1998**, *27*, 91. (c) Turecek, F. *J. Mass Spectrom.* **1998**, *33*, 779.

(14) (a) Danis, P. O.; Feng, R.; McLafferty, F. W. *Anal. Chem.* **1986**, *58*, 348. (b) Turecek, F.; Drinkwater, D. E.; McLafferty, F. W.; Maquestiau, A. *Org. Mass Spectrom.* **1989**, *24*, 669.

(15) Turecek, F.; Gu, M.; Shaffer, S. A. *J. Am. Soc. Mass Spectrom.* **1992**, *3*, 493.

(16) (a) Bateman, R. H.; Brown, J.; Lefevere, M.; Flammang, R.; Van Haverbeke, Y. *Int. J. Mass Spectrom. Ion Processes* **1992**, *115*, 205. (b) Flammang, R.; Van Haverbeke, Y.; Braybrook, C.; Brown, J. *Rapid Commun. Mass Spectrom.* **1995**, *9*, 795.

(17) Gilman, J. P.; Hsieh, T.; Meisels, G. G. *J. Chem. Phys.* **1983**, *78*, 1174.

(18) (a) Baudisch, O. *Science* **1940**, *92*, 336. (b) Baudisch, O.; Smith, S. H. *Naturwissenschaften* **1939**, *46*, 768.

(19) Frisch, M. J.; Trucks, G. W.; Schlegel, H. B.; Scuseria, G. E.; Robb, M. A.; Cheeseman, J. R.; Zakrzewski, V. G.; Montgomery, J. A., Jr.; Stratmann, R. E.; Burant, J. C.; Dapprich, S.; Millam, J. M.; Daniels, A. D.; Kudin, K. N.; Strain, M. C.; Farkas, O.; Tomasi, J.; Barone, V.; Cossi, M.; Cammi, R.; Mennucci, B.; Pomelli, C.; Adamo, C.; Clifford, S.; Ochterski, J.; Petersson, G. A.; Ayala, P. Y.; Cui, Q.; Morokuma, K.; Malick, D. K.; Rabuck, A. D.; Raghavachari, K.; Foresman, J. B.; Cioslowski, J.; Ortiz, J. V.; Stefanov, B. B.; Liu, G.; Liashenko, A.; Piskorz, P.; Komaromi, I.; Gomperts, R.; Martin, R. L.; Fox, D. J.; Keith, T.; Al-Laham, M. A.; Peng, C. Y.; Nanayakkara, A.; Gonzalez, C.; Challacombe, M.; Gill, P. M. W.; Johnson, B.; Chen, W.; Wong, M. W.; Andres, J. L.; Gonzalez, C.; Head-Gordon, M.; Replogle, E. S.; Pople, J. A.: *Gaussian 98, Revision A.6*; Gaussian, Inc.: Pittsburgh, PA, 1998.

(20) Parr, R. G.; Yang, W. *Density Functional Theory of Atoms and Molecules*; Oxford University Press: New York, 1989.

(21) (a) Becke, A. D. *J. Chem. Phys.* **1993**, *98*, 1372 and 5648. (b) Stephens, P. J.; Devlin, F. J.; Chablowski, C. F.; Frisch, M. J. *J. Phys. Chem.* **1994**, *98*, 11623.

(22) Rauhut, G.; Pulay, P. *J. Phys. Chem.* **1995**, *99*, 3093.

(23) Finley, J. W.; Stephens, P. J. *J. Mol. Struct. (THEOCHEM)* **1995**, *227*, 357.

(24) Wong, M. W. *Chem. Phys. Lett.* **1996**, *256*, 391.
(25) Scott, A. P.; Radom, L. *J. Phys. Chem.* **1996**, *100*, 16502.
(26) (a) Schlegel, H. B. *J. Chem. Phys.* **1986**, *84*, 4530. (b) Mayer, I. *Adv. Quantum Chem.* **1980**, *12*, 189.
(27) McWeeny, R.; Diercksen, G. *J. Chem. Phys.* **1968**, *49*, 4852.
(28) Parkinson, C. J.; Mayer, P. M.; Radom, L. *J. Chem. Soc., Perkin Trans. 2* **1999**, 2305.
(29) Turecek, F. *J. Phys. Chem. A* **1998**, *102*, 4703.
(30) (a) Turecek, F.; Wolken, J. K. *J. Phys. Chem. A* **1999**, *103*, 1905. (b) Wolken, J. K.; Turecek, F. *J. Phys. Chem. A* **1999**, *103*, 6268. (c) Wolken, J. K.; Turecek, F. *J. Am.* Chem. Soc. **1999**, *121*, 6010. (d) Turecek, F.; Carpenter, F. H. *J. Chem. Soc., Perkin* Trans. 2 **1999**, 2315. (e) Turecek, F.; Polasek, M.; Frank, A. J.; Sadilek, M. *J. Am. Chem. Soc.* **2000**, *122*, 2361.
(31) Rablen, P. R. *J. Am. Chem. Soc.* **2000**, *122*, 357.
(32) Abboud, J.-L. M.; Notario, R.; Yanez, M.; Mo, O.; Flammang, R.; Jagerovic, N.; Alkorta, I.; Elguero, J. *J. Phys. Org. Chem.* **1999**, *12*, 787.
(33) McLafferty, F. W.; Turecek, F. *Interpretation of Mass Spectra, 4th ed.*; University Science Books: Mill Valley, CA, 1993.
(34) Harrison, A. G. *Chemical Ionization Mass Spectrometry*, 2nd ed.; CRC Press: Boca Raton, 1992.
(35) Reents, W. D., Jr.; Freiser, B. S. *J. Am. Chem. Soc.* **1981**, *103*, 27911.
(36) Cacace, F.; de Petris, G.; Pepi, F. *Proc. Natl. Acad. Sci. U.S.A.* **1997**, *94*, 3507.
(37) Stirk, K. M.; Orlowski, J. C.; Leeck, D. T.; Kenttamaa. H. I. *J. Am. Chem. Soc.* **1992**, *114*, 8604.
(38) Kimura, K.; Katsumata, K.; Achiba, Y.; Yamazaki, T.; Iwata, S. *Handbook of He(I) Photoelectron Spectra of Fundamental Organic Molecules*; Japan Scientific Societies Press: Tokyo, 1981.
(39) Filges, U.; Grutzmacher, H.-F. *Org. Mass Spectrom.* **1986**, *21*, 673.
(40) Chou, P. K.; Gao, L.; Tichy, S. E.; Painter, S. L.; Blackstock, S. C.; Kenttamaa, H. I. *J. Phys. Chem. A*, **2000**, *104*, 5530.
(41) Grundmann, C. Ortho-Chinone. In *Methoden der Organischen Chemie (Houben- Weyl)*, Chinone II; Grundmann, C., Ed.; Thieme: Stuttgart, 1979.
(42) Brown E. R. Quinonedimines, monoimines and related compounds. In *The chemistry of the quinonoid compounds*, Vol. 2, Part 2; Patai, S., Rappoport, Z., Eds.; John Wiley and Sons: Chichester, 1988; Chapter 21, pp 1287−1289.
(43) Breuer, E.; Aurich, H. G.; Nielsen, A. *Nitrones, Nitronates and Nitroxides*; Wiley: Chichester, 1989; pp 139−244.